Cameleon imaging of calcium transients in cultured mechanosensory neurons in *Caenorhabditis elegans*

Christian Frøkjær-Jensen
Speciale
February 2003
Niels Bohr Institute
University of Copenhagen

Table of contents

Abstract

Traditional techniques to study cell function, such as pharmacology, electrophysiology and calcium sensitive dye loading, have been difficult to use in *Caenorhabditis elegans* largely because of the impermeable, pressurized cuticle surrounding the animals. We have taken advantage of recent advances in genetically encoded calcium sensors and in culture techniques to overcome some of these technical difficulties and have studied the role of voltage gated calcium channels in mechanosensory neurons.

We expressed the yellow cameleon 2.12 calcium indicator in mechanosensory neurons and studied calcium transients in primary cultures in response to transient depolarization. We found that the calcium indicator retained its function in cultured neurons and reproducible calcium transients were recorded from single neurons. Calcium transients were blocked by micromolar concentrations of L-type calcium channel blockers verapamil, diltiazem and nifedipine, indicating a role for voltage gated calcium channels in generating transients. We performed experiments on voltage gated calcium channel α_1-subunit mutants, *unc-2(lj1)* and *egl-19(ad1006)* and with $\alpha_2\delta$ subunit mutant *unc-36(e251)*. Transients were significantly reduced in cultured neurons from *egl-19(ad1006)* and *unc-36(e251),* whereas we could not detect a significant reduction in the *unc-2(lj1)* background, nor in the ryanodine receptor mutant *unc-68(r1158)* or the IP_3-receptor mutant *itr-1(sa73).* Promoter driven GFP expression confirmed UNC-36 was the only $\alpha_2\delta$ subunit expressed in the mechanosensory neurons.

We also performed an *in situ* calibration of yellow cameleon 2.12. The sensor showed a biphasic calcium dependence with apparent EC_{50} values of 0.4μM and 40 μM,

respectively and a dynamic range of 81 +- 2 % (n = 12). Based on this calibration we estimate that the cultured mechanosensory neurons had a resting free calcium concentration of approximately 200 nM.

Combined with the lack of putative voltage gated Na^+ channels in the *C.elegans* genome, these experiments suggest a central role for EGL-19 and UNC-36 in excitability of the mechanosensory neurons. Also, we have shown that genetically encoded calcium sensors and cultured neurons are useful new tools for studying protein function in *C.elegans*.

Credit

I could not have undertaken this project without the help from everyone in the Schafer lab and much of the work has a collaborative nature. For clarity, I will describe here the specific parts contributed to this thesis by others in the lab.
Dr. Rex Kerr initiated the development of the cameleon imaging technique in *C.elegans*. He assembled the imaging rig and he wrote the image analysis and the data analysis software used for this project. I have subsequently modified the analysis software in Matlab to handle the specific type of data that I collected. Dr. Hiroshi Suzuki made the strain expressing the cameleon construct in the mechanosensory neurons. He also made the *itr-1(sa73)* cameleon strain. Dr. Massimo Hilliard and Katie Kindt scored the expression patterns of the transgenic worms.

Introduction

C.elegans as a model system

Sydney Brenner originally adopted *Caenorhabditis elegans* as a model organism in 1965 hoping to characterize animal development and the relationship between behavior and nervous system function (Riddle, 1997) and was awarded the 2002 Nobel Prize in medicine, together with Dr. Horwitz and Dr. Sulston, for their work on programmed cell death. *C. elegans* is a 1.5 mm long nematode with a 2-3 day reproductive life cycle that is very amenable to genetic analysis. *C. elegans* has two sexes. Hermaphrodites (two X chromosomes) are self fertilizing which makes viability and maintenance of even severe mutants relatively simple. Stocks can be kept for at least 25 years frozen in liquid nitrogen, minimizing problems associated with spontaneous mutations. Rare males (one X chromosome) result from chromosomal non-segregation (or male fertizilation) and are particularly useful for generating combinations of mutant alleles. The animals are easily maintained at room temperature and grown in petri dishes on nematode growth media (NGM) seeded with *Escherichia coli* as the food source.

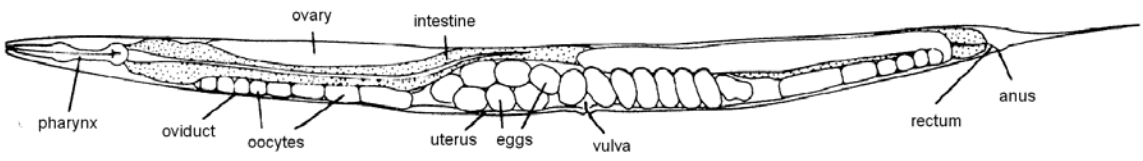

Fig.1. Schematic figure of *C.elegans* hermaphrodite. Image from Riddle et al. (1997)

The *C. elegans* genome is fully sequenced and consists of approx. 19000 genes, many with high similarity to vertebrate genes (Bargmann, 1998 and C. elegans consortium, 1998). Among the conserved gene families are those involved in synaptic release mechanisms, neurotransmitter receptors, neurotransmitter biosynthetic enzymes, second messenger pathways and ion channels (Bargmann, 1998).

The hermaphrodite nervous system is relatively simple and very well characterized. The entire nervous system consists of 302 neurons with fixed positions and the synaptic connections between neurons have been fully mapped at the electron microscopy level (White et al., 1986). In spite of its simple nervous system, *C.elegans* displays a range of different behaviors such as chemotaxis towards food, thermotaxis toward culturing temperature, habituation to mechanical, chemical and noxious stimuli and associative learning to food or starvation paired with the presence of specific ions(*C. elegans* II, 1997) [specifically Jorgensen, E.M, and Rankin, C., "Neural Plasticity", pp. 769-790]. The invariant neuron location combined with the transparency of the worm has made the analysis of single neuron function possible by neuron specific laser ablation.

Unfortunately, traditional techniques such as electrophysiology, pharmacology and use of indicator dyes are time consuming and technically difficult in intact worms, mainly because of the tough impermeable cuticle surrounding the worm. We will describe how recent advances in primary cell culturing and genetically encoded calcium sensors can be used to overcome some of these technical difficulties and provide insight into the role of voltage gated calcium channels and intracellular calcium release in mechanosensory neurons.

Vertebrate voltage gated calcium channels

Voltage gated calcium channels (VGCCs) play a central role as the link between electrical signaling and many important cellular processes. Electrical signaling, in the form of changes in potential across the cell membrane, can open voltage gated calcium selective ion channels. Entering calcium functions as a second messenger and can initiate neurotransmitter release from nerve terminals, muscle contraction through excitation-contraction coupling and longer lasting effects on gene expression (for a review see Catterall, 2000).

Vertebrate VGCCs typically consist of the pore forming α_1 subunit and the regulatory subunits β, $\alpha_2\delta$ and γ. The α_1 subunit is a membrane spanning protein with a pore forming structure in the center which, when open, selectively allows Ca^{2+} ion flux across the membrane. The Ca^{2+} flux is inward because of the low intracellular calcium concentration (approx. $10^{-7} – 10^{-6}$ M) compared to the millimolar extracellular concentration. The ion channel is composed of four repeated domains (I-IV), each consisting of six transmembrane segments (S1-S6) (see fig.2). The S4 segment has regularly spaced positive amino acids, allowing the segment to function as a membrane voltage sensor. In response to membrane depolarization the S4 segment moves and the channel changes to an open conformation.

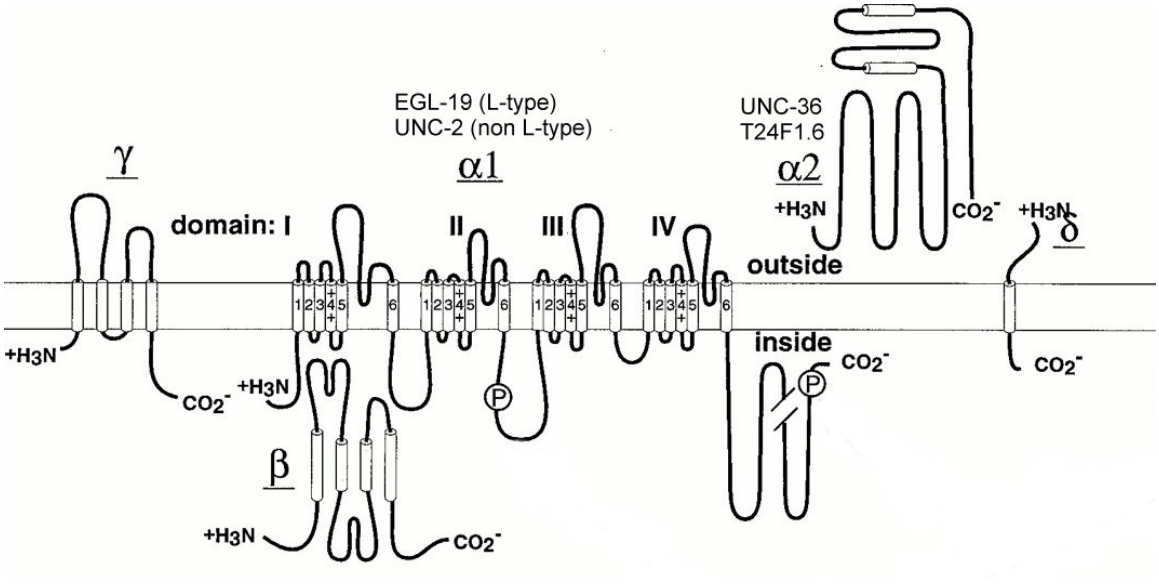

Fig. 2. Schematic depiction of voltage gated calcium channel subunits. EGL-19, UNC-2, UNC-36 and T24F1.6 refer to *C.elegans* homologs of these subunits. Modified from Catterall (2000).

The S5 and S6 segments, and the membrane associated loop between them, line the inside of the pore. Each domain contains a membrane associated loop with a pair of glutamate residues that confer the calcium ion specificity (Catterall, 2000).

Vertebrate α_1 subunits are classified based on similarity among genes, activation threshold and pharmacological properties. Channel activation threshold divides the channels into high voltage activated (HVA) and low voltage activated (LVA) channels. The HVA channels typically have the subunit composition discussed above, whereas the LVA channels do not necessarily have subunits associated. The HVA channels are further classified based on susceptibility to blockers. L-type channels are dihydropyridine (DHP) sensitive HVA channels. L-type channels are also blocked by phenylalkylamines and benzothiazepines, which bind to distinct but overlapping residues (Striessnig et al., 1998 and Hockerman et al., 2000). The L-type calcium channel currents are further

distinguished by inactivating very slowly (τ >500 msec) as opposed to the faster LVA and non-L type channels ($\tau \approx$ 50msec) (Hille, 1992). HVA channels that are not blocked by DHPs are classified as non-L type. Non L-type channels can be further classified into N, P/Q and R type based on differential block by peptide toxins.

The regulatory subunits are not strictly necessary for α_1 channel function but enhance the expression level of channels, single channel conductance and change activation/inactivation parameters (Singer et al., 1991). The β subunit is particularly important for α_1 function in neurons, whereas β, $\alpha_2\delta$ and γ have been shown to be functionally important in muscles (Catterall, 2000). The β subunit is intracellular with no transmembrane segments. In contrast, the α_2 is located extracellularly and is heavily glycosylated. The α_2 subunit is tethered to the membrane with disulfide bonds to the membrane-spanning δ subunit. The α_2 and δ subunits are encoded by the same gene which undergoes post-translational cleavage and relinking by disulphide bonds (Jay et al., 1991). The γ subunit spans the membrane and has been implicated in enhancing steady state channel inactivation in mice (Letts et al., 1998).

$\alpha_2\delta$ has specifically been shown to enhance L-type channel expression in HEK 293 cells (Bangalore et al., 1996). Several studies show the expression of $\alpha_2\delta$ in neurons (Klugbauer et al., 1999, Brodbeck et al., 2002 and Sutton et al., 2002) and both the $\alpha_2\delta$ and the γ subunit have been implicated in epilepsy. Gabapentin, an antiepileptic drug, is reported to act by binding to the $\alpha_2\delta$ subunit (Gee *et al*., 1996 and Letts et al., 1998). The role of $\alpha_2\delta$ in neurons however has only recently been characterized functionally. Mice deficient in the $\alpha_2\delta$-2 channel subunit (ducky mutation) are used as a model for absence

epilepsy and have altered Purkinje cell morphology. Coexpression of the mutated $\alpha_2\delta$-2 channel also reduces peak calcium current density (Brodbeck et al., 2002). This indicates a negative effect of the mutated subunit, rather than just an effect of lacking the subunit.

In summary in vertebrates different types of pore forming α_1 subunits regulate calcium influx into cells in response to depolarization. The α_1 subunits can be distinguished by different sensitivity to pharmacological blockers and β, $\alpha_2\delta$ and γ subunits can modulate functional aspects of the channels.

Invertebrate voltage gated calcium channels

Invertebrate VGCCs have not been as extensively characterized as vertebrate calcium channels (for a review see Jeziorski et al., 2000). Some of the defining characteristics of vertebrate VGCCs, such as antagonist sensitivity, are not necessarily conserved in invertebrates. For example, an α_1 subunit isolated from the jellyfish *Cyanea* is structurally similar to mammalian L-type channels but is insensitive to DHPs and peptide toxins (Jeziorski et al., 1998). To avoid ambiguity, Jeziorski et al. (2000) have proposed to adopt a molecular definition of channel subtype, as the antagonist binding residues typically account for small regions of the channel, whereas the overall channel structure is more relevant for the functional aspects of the channel.

The *C.elegans* genome contains three genes with similarity to known vertebrate VGCCs. EGL-19, UNC-2 and CCA-1, encode an L-type, non L-type and a LVA T-type channel, respectively. Two additional genes resemble voltage gated channels with a similar four domain structure, but the functional role of these two putative channels has

not been determined and no mutants have been mapped to these locations (Jeziorski et al., 2000).

The role of EGL-19 in the pharyngeal muscles has been studied by several groups. Initial characterization and mapping of the gene was described by Lee et al.(1997). The authors demonstrated the effect of gain of function alleles and loss of function alleles on electropharyngeograms (EPGs). EPGs are the equivalent of an electrocardiogram on *C.elegans*, where current passing through the mouth as a result of pharyngeal pumping is measured with an extracellular electrode. EGL-19 was shown functionally to be the main voltage gated calcium channel responsible for pharyngeal muscle depolarization. However, expression pattern analysis with a partial protein::GFP fusion showed expression in unidentified neurons as well as muscle. Also, analysis of dauer formation (a dormant state *C.elegans* enters in the absence of food) led the authors to suspect a possible role in neurons. EGL-19 was further characterized with the genetically encoded calcium indicator cameleon (Kerr et al., 2000) by studying calcium transients in the pharynx *in vivo*. Loss of function allele *egl-19(ad1006)* showed a 19% decrease and the gain of function allele *egl-19(n2368)* a 19 % increase in calcium ratio amplitude, confirming the functional role of EGL-19 in pharyngeal muscle.

The role of UNC-36, which encodes one of two putative *C.elegans* $\alpha_2\delta$ subunits was also investigated. Surprisingly, *unc-36(e251)* loss of function mutants showed steeper calcium transients than wildtype, indicative of a higher calcium flux. Based on vertebrate characterization (Bangalore et al., 1996) one would expect a non-functional $\alpha_2\delta$ subunit to decrease the amplitude and sharpness of calcium transients. There is some

evidence that suggests that UNC-2 and UNC-36 both play an important role in neurotransmitter release at the synapse (Schafer et al., 1996).

The functional role of VGCCs in *C.elegans* is especially interesting because of the apparent lack of voltage gated Na^+ channels, which play an important role in action potential initiation in vertebrates. *C.elegans* neurons are believed to be non-spiking and communicate by graded potentials (Thomas and Lockery, 1999). Neurons have a high input resistance and display a regenerative calcium current leading to a high sensitivity to sensory or synaptic input (Goodman et al., 1998). The resting membrane potential in at least two chemosensory neurons (AWA and AWC) has been measured to -20 mV, which is considerably less negative than vertebrate neurons (-70mV) (Nickel et al., 2002). This finding is surprising and, if true, would suggest that the resting membrane potential is not necessarily dominated by the K^+ conductance.

The recent discovery of a voltage gated bacterial Na^+ channel (NaChBac) with only one 6TM domain and more similarity to Ca^{2+} channels than Na^+ channels (Ren et al., 2001) forces one to reconsider the apparent lack of voltage gated Na^+ channels in *C.elegans*. The existence of a voltage gated Na^+ channel in *C.elegans* muscle has recently been proposed by Franks et al. (2002) based on intracellular recordings from the pharynx, but this finding has yet to be confirmed by other groups.

C.elegans has homologs of all the major types of VGCCs and the associated subunits. These VGCCs have been studied in muscle but not much is known about their functional role in neurons. VGCCs have been proposed to be particularly important in *C.elegans* because there are no obvious voltage gated Na^+ channel genes. We would like

to characterize the functional role of VGCCs in *C.elegans* neurons and their pharmacological properties.

Cameleon indicator

Dr. Tsien and colleagues have developed genetically encoded calcium sensitive indicators based on Fluorescence Resonance Energy Transfer (FRET) (Miyawaki et al., 1997, Miyawaki et al., 1999). Briefly, FRET involves the non-radiative energy transfer between two fluorophores. This process is highly dependent on the distance and relative orientation of fluorophores, with the biologically relevant interaction distance on the order of 5-10 nm. The calcium sensors were called cameleons because they are based on calmodulin (CaM) and sense calcium changes by changing the relative emission of two different color wavelengths. CaM is a small, 150 amino acid protein with 4 calcium binding sites, organized in two domains with different calcium binding affinities. The protein has no catalytic action itself, but works by changing conformation in response to calcium concentration and thereby activates a long list of kinases.

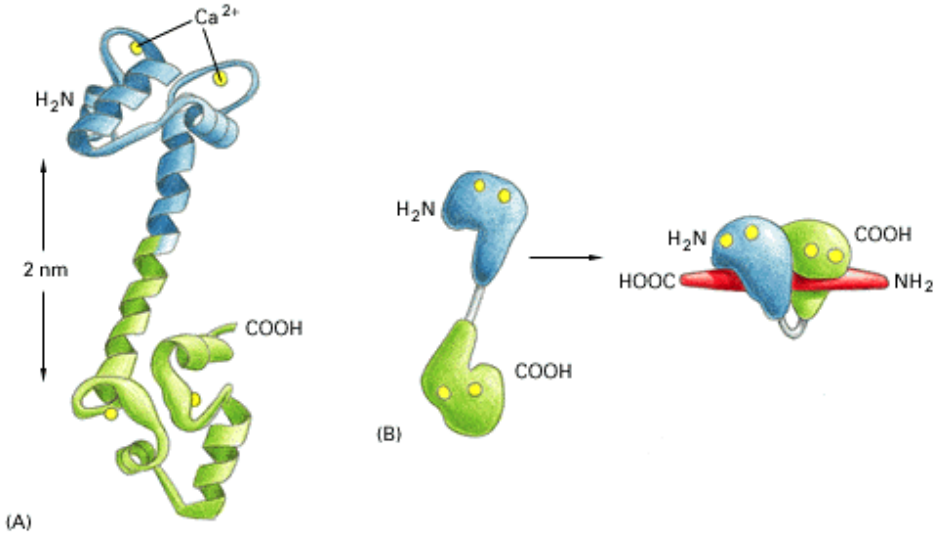

Fig. 3. Schematic of calmodulin action.
(A) Shows the ribbon depiction of the protein in its unfolded state.
(B) Shows the conformational change after binding calcium and CaM interaction with a CaM binding domain.
Figure from Molecular biology of the cell, 3rd ed.

The cameleon proteins were engineered to take advantage of the conformational change in response to calcium concentration. The sensor consists of two fluorophores, cyan fluorescent protein (CFP) and yellow fluorescent protein (YFP), linked by CaM and the calmodulin binding peptide M13. CFP can be selectively excited with appropriate filters and in low calcium surroundings cameleon will be in its most open conformation, positioning the two fluorophores far from each other and resulting in low FRET efficiency and a high CFP emission. In high calcium, CaM binds to M13 and the two fluorophores are brought closer together, enabling FRET and resulting in an increased YFP emission at the expense of CFP emission (fig. 4).

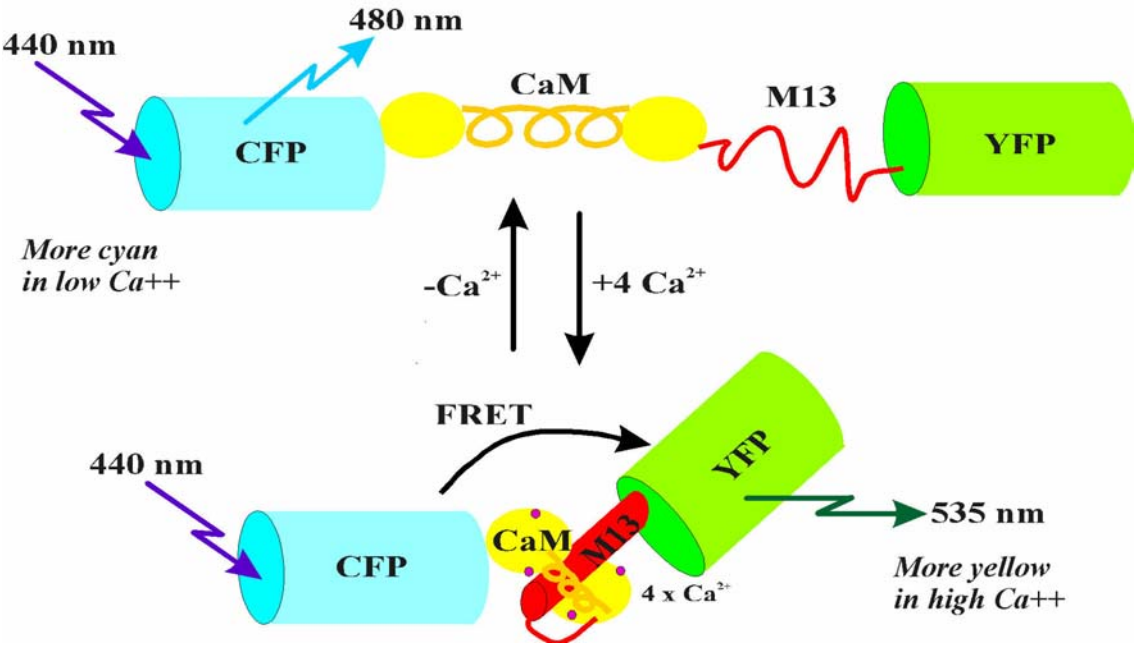

adapted from Miyawaki A, *Nature*

Fig. 4. Schematic of cameleon function

Upper part shows the cameleon protein in low calcium surroundings with the two fluorophores positioned far apart. Lower part shows conformational change induced in high calcium surroundings.

We use these reciprocal changes in fluorescence as a measure of changes in calcium concentration. The ratio between YFP and CFP is a better measure of calcium concentration changes than the individual intensities, since the ratio reduces signal dependence on indicator concentration. Also, movement artifacts and lamp instability fluctuations effectively cancel out (Kerr, 2002).

Earlier work in our lab had shown that yellow cameleons could be used successfully in muscles in intact animals to study the effects of disrupted ion channel function (Kerr et al., 2000). Unfortunately, the small size of *C.elegans* neurons (approx. 5

μm diameter) and difficulty in delivering a well defined stimulus made successful neuronal recordings more difficult. Recordings from populations of neurons in the nerve ring in response to rather crude whole animal stimulation with electrical shock showed the expected ratio increase, but single neuron recordings were unsuccessful at the time.

Mechanosensory neurons and primary culture

C.elegans has been used extensively to study mechanosensory channels at the behavioral, genetic and electrophysiological level (review Tavernarakis and Driscoll, 1997). Behaviorally, *C.elegans* responds to anterior touch by backing away from the touch and to posterior touch by speeding up. 5 mechanosensory neurons, AVM, ALML/ALMR (anterior part of the worm) and PLML/PLMR (posterior part) are responsible for sensing touch. PVM is also categorized as a mechanosensory neuron based on morphology and gene expression, although laser ablation studies have shown that the neuron is not essential for touch sensitivity. At least 16 genes involved in cell specification or mechanotransduction have been isolated (Tavernarakis and Driscoll, 1997). Of these, MEC-4 and MEC-10 encode the putative mechanosensitive channel proteins, MEC-2 is involved in linking the channel to the cytoskeleton and MEC-12 and MEC-7 encode tubulins needed for intracellular microtubule formation. MEC-4 is only expressed in the 6 mechanosensory neurons mentioned above.

We chose to use the mechanosensory neurons because they constitute a well defined subset of neurons with a similar functional role. Also, we were interested in comparing results obtained in culture with simultaneous experiments carried out *in vivo*, where mechanosensory stimuli allowed for good activation of single neurons.

Recently, techniques were developed for making primary cultures of *C.elegans* cells (Christensen et al., 2002). Primary cultures of single cells isolated from *C.elegans* embryos differentiated in culture into cells with both neuronal and muscular morphology. Cultured cells were shown to retain many of their *in vivo* characteristics when cultured, such as morphology and cell fate based on relative abundance of GFP tagged cells. The cultured cells are thought to differentiate into the various cells that are present in the newly hatched L1 larva, although this still needs further study. Christensen et al. (2002) showed that a strain expressing GFP in the mechanosensory neurons clearly differentiated into bright cells with neuronal morphology and extensive processes. It should be noted though, that the GFP labeled mechanosensory neurons were expressed at a higher frequency than expected from the number of mechanosensory neurons present in the L1 animal (the 4 mechanosensory neurons ALML/ALMR and PLML/PLMR).

We reasoned that the primary culture system could overcome some of the problems associated with intact worms and allow us good control of stimuli and pharmacological manipulations. The genetically encoded calcium indicators made it possible to restrict the experiments to a small and well defined population of neurons thereby reducing variability and making comparisons with *in vivo* studies of gene expression possible.

Results

Calibration of cameleon in cultured *C.elegans* neurons

We prepared *C. elegans* primary cultures from a strain expressing cameleon YC2.12 under the *mec-4* promoter in the mechanosensory neurons and cameleon expression in the mechanosensory neurons was confirmed by Nomarski microscopy. We followed the protocol described by Christensen et al. (2002), with only small modifications (described in the materials section). Cell cultures were healthy with clearly differentiated muscle and neuronal cells, with a subset of the neurons expressing the cameleon protein. Cameleon expression increased during the first two days. Fig. 5A shows a photo of 3 day old cultures, with 7 neurons expressing YC2.12 (bright cells).

Collaborators in professor Driscoll's lab have cultured mechanosensory neurons expressing GFP under the *mec-4* promoter and these bright neurons retained many of their *in vivo* properties when cultured. The morphology of cultured neurons matched the *in vivo* morphology of mechanosensory neurons. Also, the characteristic necrosis of mechanosensory *mec-4(d)* neurons was replicated in culture (pers. comm. L. Bianchi). These controls convinced us that the mechanosensory neuron specific promoter *mec-4* retained its specificity in cultured neurons.

We recorded on a Zeiss Axioskop 2 compound microscope with a wide field emission splitter allowing us to make simultaneous measurement of cyan and yellow emission intensities on a single ccd chip (previously described in Kerr et al., 2000). We analyzed images with custom software. This software computed the yellow and cyan emission intensities in streams of images to produce a record of ratio change over time.

For the long calibration measurements we recorded at 0.2 Hz with a shutter to minimize the bleaching of sample over time and for the much shorter depolarization experiments we recorded at 10 Hz without the shutter to increase temporal resolution. Data is tabulated in appendix I and all values in the text are specified as mean +- standard error of mean (independent trials).

We performed an *in situ* calibration of the cameleon protein to determine the dynamic properties of the sensor in a cellular environment. As discussed by Neher (1995) there are several reports of small molecule calcium indicators having altered dynamic properties *in vivo* compared to *in vitro* characterizations. Such changes of dynamic range and apparent dissociation constants are presumably due to factors such as sensor interaction with endogenous proteins and quenching of signals by other cellular proteins. This discussion does not necessarily apply to the larger protein based cameleon indicator although there have been reports of poor cameleon function when expressed transgenically in mice hippocampal neurons (T.Knöpfel, pers. comm.). Furthermore, no *in vitro* or *in situ* calibration results have previously been published on the yc2.12.

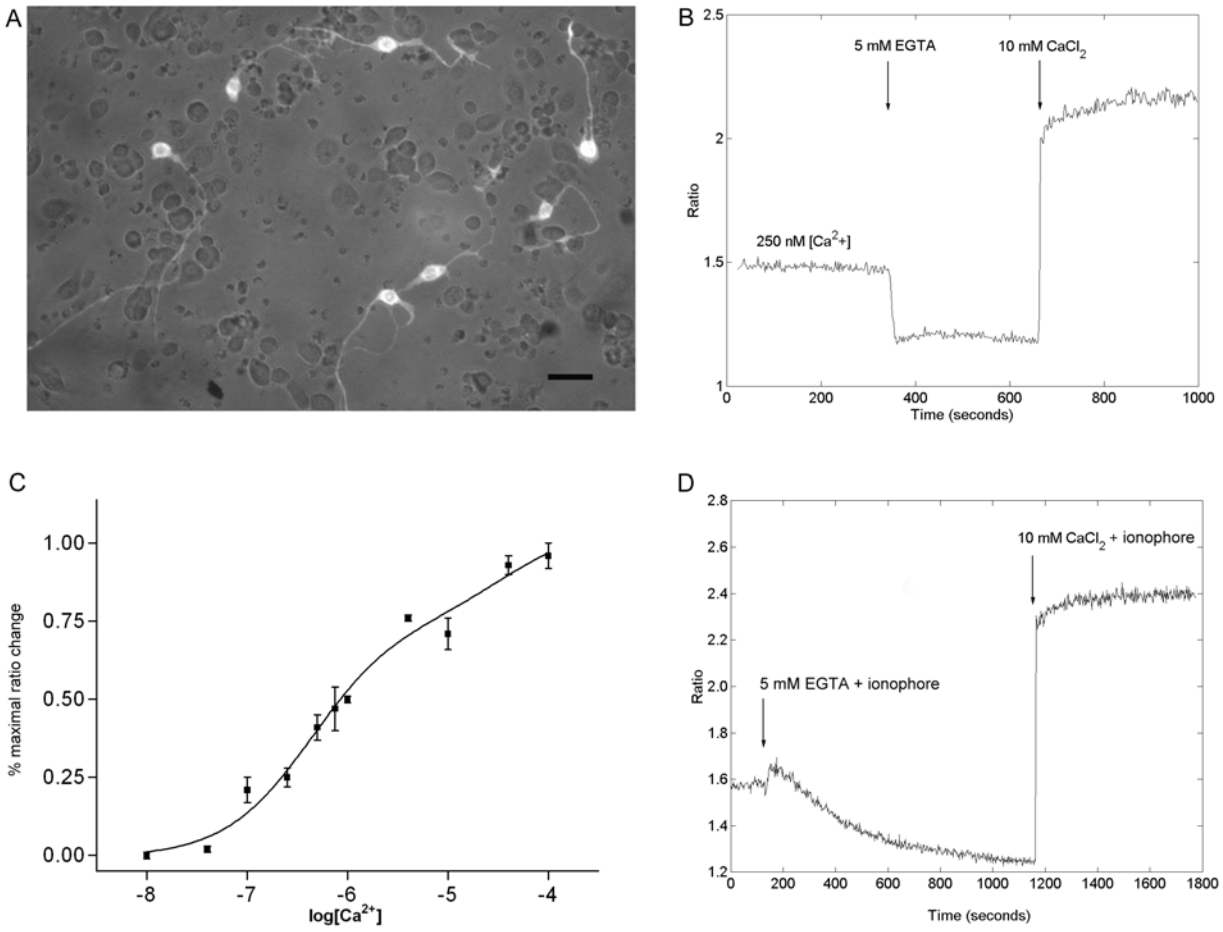

Fig. 5. Calibration of yellow cameleon 2.12 in cultured neurons.

(A) Primary *C.elegans* culture of the strain bzIs18 which expresses yellow cameleon 2.12 (yc2.12) in the mechanosensory neurons. Picture is taken 3 days after culturing and shows differentiated neurons expressing cameleon protein (bright neurons). All neurons expressing cameleon show neuronal morphology. Scale bar 10 micron.

(B) Representative trace from cameleon calibration in cultured neurons. Prior to recording cultures were incubated 25-30 minutes in a solution with a well defined concentration of free calcium in the presence of the calcium ionophore Br-A23187 (10 μM). The solution also contained Rotenone (10mM) and 2-deoxy-D-glucose (1.8mM) to block active pumps.

(C) Yc2.12 calibration curve showing the aggregate results from 11 different free calcium solutions. Ratio is normalized to the maximal ratio change for the individual cell. A biphasic calcium dependence gave the best fit, with apparent EC_{50} values of 0.4 μM and 40 μM. The maximum/minimum ratio change was 81 +- 2 % (n = 12).

(D) Estimate of the intracellular calcium concentration in cultured neurons. Cultured neurons were imaged 3 minutes in a standard extracellular saline solution. 5 mM EGTA, ionophore, Rotenone and 2-deoxy-D-glucose were added to determine the minimum ratio and 10 mM $CaCl_2$, ionophore and metabolic blockers added to determine the maximum ratio value. Resting ratio in cultured neurons was measured to 22 +- 7 % (n = 2, 18 cells) of maximal ratio change corresponding to a calcium concentration of approx. 200 nM.

Following a protocol described by Thomas et al. (2000) we measured the fluorescent ratio changes of cameleon with commercially available calcium buffers containing free calcium in the range from 10nM to 100 μM in the presence of 10 μM of the non-fluorescent calcium ionophore Br-A23187. Cultured cells were washed with extracellular saline twice and then placed in a calcium buffered solution containing 10 μM Br-A23187, Rotenone (a mitochondrial inhibitor) and 2-deoxy-D-glucose (an anti-metabolite). Including Rotenone and 2-deoxy-D-glucose effectively blocks the cell's energy production and was necessary to obtain stable baseline ratios at low calcium concentrations. Presumably, this blocks the effect of active calcium pumps in the membranes. After 15-20 minutes of equilibration the cells were transferred into fresh calcium buffer in the recording chamber. We measured the fluorescence ratio for 5 min. at a given calcium concentration followed by 5 minutes in nominally 0mM Ca^{2+} (5mM EGTA) and 5 minutes in high calcium (10 mM Ca^{2+}). Cells were flushed with nominally calcium free extracellular saline between solution changes to avoid large pH changes associated with EGTA binding free calcium.

Fig.5B shows a typical example of a ratio trace, here obtained with a 250 nM free calcium buffer. Ratio changes are relatively quick (within the first 4-5 time points = approx. 20 seconds), indicating rapid equilibration of calcium concentrations with the cell cytoplasm. Similar traces with three stable plateaus were obtained for all calcium concentrations.

The cameleon calibration curve based on these experiments is shown in fig. 5C. The curve was best fit by a biphasic two site binding curve with apparent EC_{50} values of 0.4 μM and 40 μM, although the second EC_{50} value was associated with a large uncertainty

(+- 1 order of magnitude). The dynamic range of cameleon *in situ* was 81 +- 2 % (n = 12). These values compare well with the published *in vitro* calibration of yc2.1 (Miyawaki et al., 1999). We also did the *in vitro* calibration of yc2.12 on purified protein and saw a 95% ratio change (data not shown).

To determine the resting calcium level for cultured mechanosensory neurons we imaged neurons in extracellular saline for three minutes before determining the maximum ratio and minimal ratio as above. The initial calcium ratio was recorded in the absence of energy blockers, which were added together with EGTA and ionophore. The neurons had a resting cameleon ratio of 0.22 +- 0.07 % (2 dishes, 18 cells total) of maximal ratio change, corresponding to an apparent free calcium concentration of approx. 200 nM. This is, to our knowledge, the first attempt to determine the intracellular calcium concentration of cultured *C.elegans* neurons.

The calibration results convinced us that the cameleon indicator functioned properly in cultured neurons and could be used as a reliable measure of changes in calcium concentration. To study the function of VGCCs we proceeded to test if depolarizing the neurons would induce intracellular changes in calcium concentration.

Calcium transients in response to depolarization

We tested the cultured neurons' response to depolarization and the effects of pharmacological VGCC blockers and mutations in VGCCs and subunits. We depolarized the cultured neurons transiently with an extracellular solution containing a high concentration of K^+. The protocol had previously been used with success under similar conditions to characterize the effect of drugs that bind to the $\alpha_2\delta$ subunit in rat (Martin et

al., 2001 and Sutton et al., 2002). Changing the extracellular K^+ concentration depolarizes the cell by changing the reversal potential of K^+ by:

$$\Delta E_{rev,K^+} = E_{rev,K^+}(stimulus) - E_{rev,K^+}(bath) \approx 25mV \cdot \ln\left(\frac{[K^+]_{(stimulus)}}{[K^+]_{(bath)}}\right),$$

at 20°C and assuming the intracellular K^+ concentration does not change during the stimulus. As previously mentioned, the K^+ conductance is not necessarily as dominating at rest as is commonly assumed in vertebrate neurons so the change in K^+ reversal potential is at best a rough indication of the relative depolarization with different K^+ concentrations. This estimate also does not consider the regenerative effect of opening VGCCs in the membrane, which would further depolarize the neurons. We used K^+-concentrations of 20, 40, 60, 80 and 100 mM corresponding to changes in reversal potential of 34, 51, 62, 69 and 75 mV, respectively.

We perfused cultured neurons for 8 seconds with the extracellular solution containing a high concentration of K^+ to determine the cameleon ratio change. The neurons displayed a large transient increase in cameleon ratio in response to 100 mM K^+. Fig.6A shows the response of 6 neurons imaged simultaneously from the same culture plate. All imaged neurons show a robust increase in ratio of homogenous size and similar time course, coinciding with the depolarization. Bleaching was minimized by using neutral density filters limiting the intensity of the excitation light and multiple 25 second recordings of a sample were possible without loss of indicator intensity. Perfusion with 100 mM K^+, or any of the other K^+ concentrations used, did not change the focal plane or disturb the position of the neurons.

To control for artifacts we also monitored the individual yellow and cyan emission intensities. In fig. 6B the upper trace of fig.6A is shown in detail with the

individual yellow and cyan emission intensities. The ratio faithfully reflects reciprocal changes in yellow and cyan intensities as expected from a rise in intracellular calcium.

The ratio only slowly returns to the baseline level after termination of the depolarizing stimulus. We do not currently know if this is a real measure of the calcium dynamics in *C.elegans* or if this is a property of the cameleon sensor. It does not seem to be an artifact of the cultured neurons though, since *in vivo* recordings from intact animals of the mechanosensory neurons show the same characteristic slow return to baseline calcium levels following tactile stimulation (Hiroshi et al., submitted).

We empirically measured the ratio change induced by different K^+ concentrations, to determine a useful range. As fig.6C shows, 100 mM K^+ resulted in ratio changes of 67+-1 % (n = 34), whereas 40 mM K^+ and 60 mM K^+ resulted in 32+-7 % (n=12) and 51 +-4 % (n = 6) respectively. At low K^+ concentrations, such as 20 and 40 mM, there were a large number of non-responsive cells. For 100 mM K^+ depolarization only 3 out of 307 cells did not respond. For all experiments with 20, 40 and 60 mM K^+ concentrations, initially nonresponsive cells that did respond to a subsequent 100 mM K^+ were discarded from the experiments. Most frequently, cells that did not respond to low K^+ concentrations would respond normally to 100 mM K^+ concentrations.

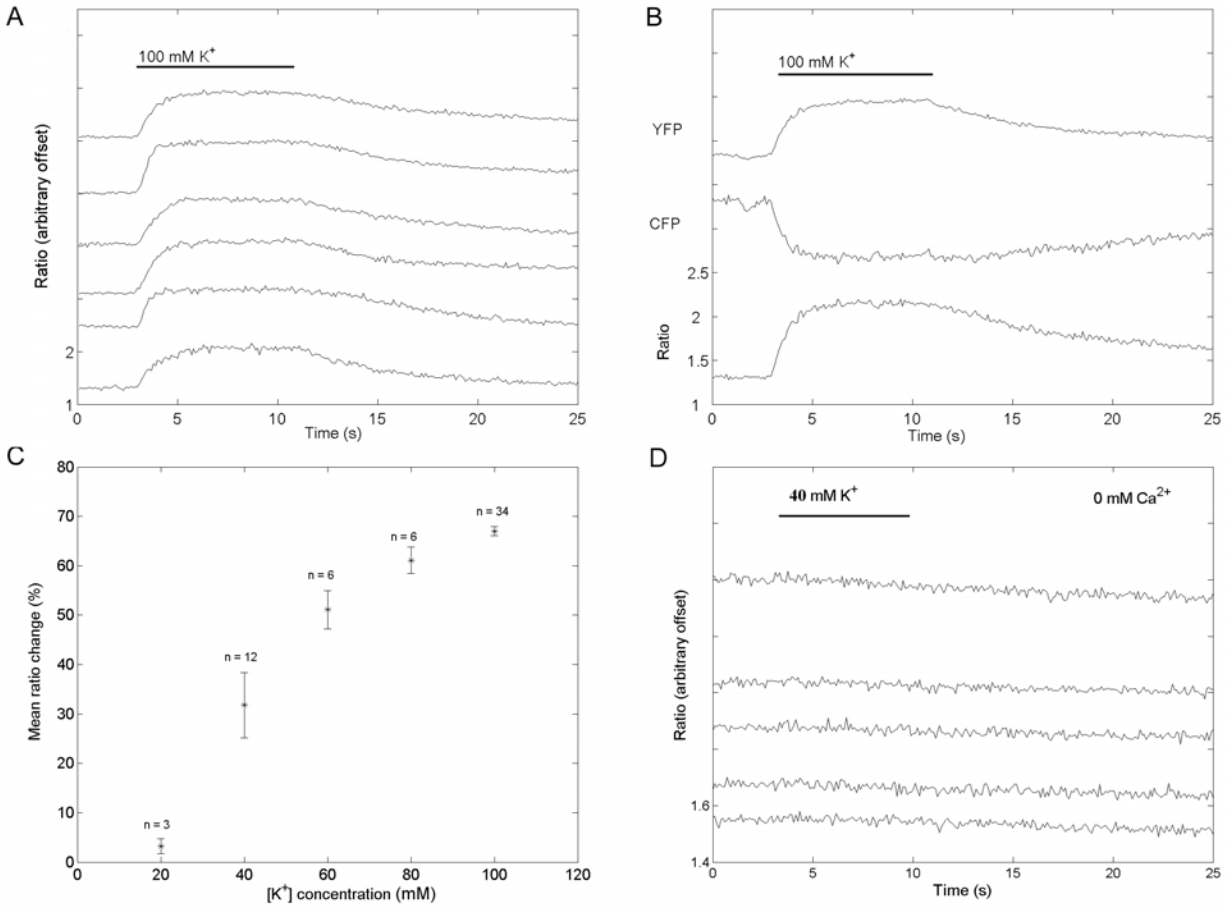

Fig.6. Depolarization of cultured neurons with high K^+ concentration

(A) Each trace shows the response of an individual neuron to a 8 s depolarization with extracellular saline containing 100 mM K^+, substituted for Na^+ in the extracellular solution. All six neurons respond to the high K^+ solution with robust increases in the cameleon ratio. An arbitrary offset has been added to the traces to facilitate viewing and only the bottom trace displays the unscaled ratio values.

(B) Upper trace from (A) shown in detail. The top traces show the individual YFP and CFP intensities and the bottom trace the ratio YFP/CFP. The ratio faithfully records the reciprocal ratio change in the individual intensities. Spikes in YFP and CFP intensities (such as the one immediately preceding the transient) reflect lamp instability and are effectively canceled out in the ratio.

(C) Transient amplitude dependence on K^+ concentration in the extracellular solution. The dependence on K^+ concentration reflects both changes in transient amplitude and number of non-responsive cells.

(D) Depolarization with 40 mM K^+ in the absence of extracellular calcium (2mM EGTA). No transients are evoked. Subsequent stimulation in the presence of 2 mM extracellular Ca^{2+} produced normal transients.

We also tested the calcium transient dependence on extracellular calcium concentration to help determine the source of calcium. Calcium transients were completely abolished in nominally calcium free depolarizing solutions (2 mM EGTA added to 40 mM K^+ solution without calcium), indicating a role for extracellular calcium as at least a partial source for calcium transients (fig. 6D). 0.5 mM calcium in the depolarizing solution restored the transients to approx. half the amplitude of the standard 2 mM Ca^{2+} concentration. Further increasing the extracellular Ca^{2+} concentration to 5 mM did not increase transient amplitude (data not shown.).

Interestingly, neurons infrequently displayed what appears to be spontaneous activity (fig. 7). This neuron displayed 4 rapid calcium increases, independent of the K^+ stimulus, which it did not respond to. In the following K^+ depolarization 2 minutes later, the neuron responded normally to the stimulation and did not show spontaneous activity. The very clear reciprocal individual intensity changes argue for the occurrence of real calcium transients. In another instance of spontaneous activity, the neuron responded normally to the K^+ stimulus and had spontaneous activity overlaid (not shown).

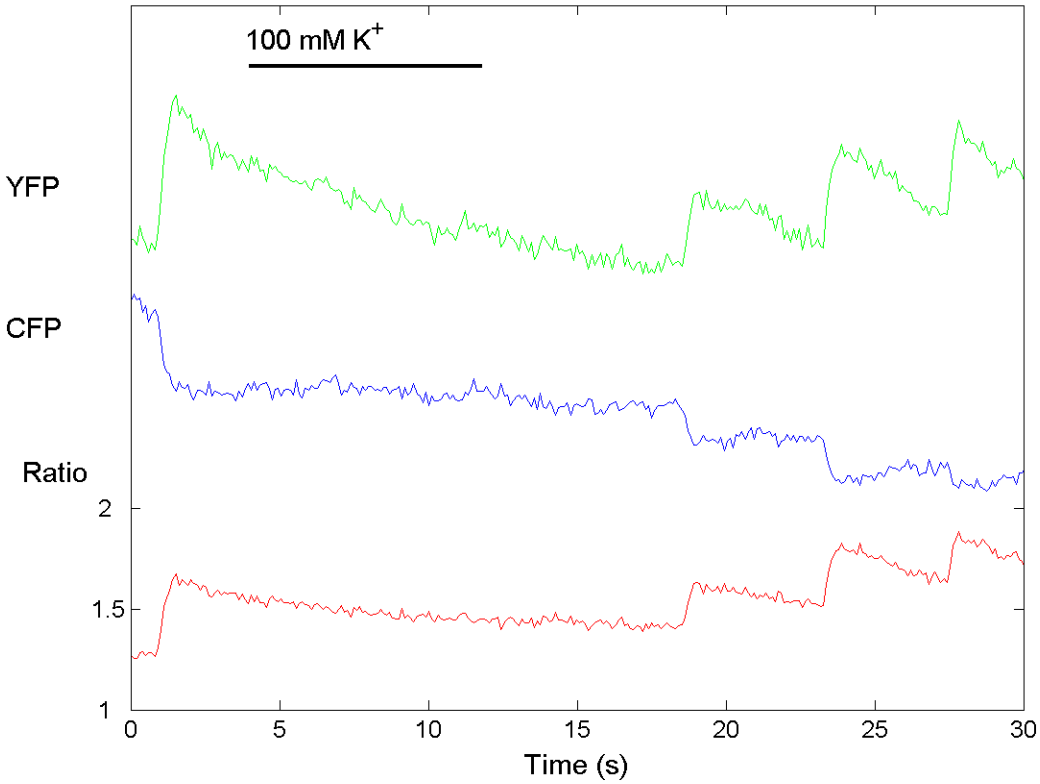

Fig. 7. Spontaneous activity in cultured mechanosensory neurons

The bottom trace shows one of the very rare instances where we observed what appears to be spontaneous activity in a cultured neuron. Surprisingly, the neuron did not respond to the applied stimulus. In the following experiment no spontaneous transients were apparent, but the cell responded to the stimulation. The very clear reciprocal changes in YFP and CFP lead us to believe that the cameleon ratio changes reflect real changes in calcium concentration.

We were content that we could reproducibly depolarize neurons and measure increases in intracellular calcium concentration. Removing extracellular calcium abolished calcium transients in response to depolarization, which led us to believe that at least part of the intracellular rise in calcium was due to calcium entering the cell through VGCCs. In order to pinpoint the molecular identity of these channels we turned to characterizing the calcium transients pharmacologically.

Pharmacological block of calcium transients

As a prerequisite for testing the effect of a given drug we first determined the reproducibility of transients in response to multiple stimulations. Fig.8A shows the average cameleon transient amplitude in response to three successive stimulations of cultured neurons with 100 mM K^+ and 2 minutes interval between stimulations. The response clearly attenuated for each successive trial. Varying stimulus length (1-10s), inter stimulus time (1-10 min) and K^+ concentration (20-100 mM) did not abolish attenuation of amplitude. The attenuation should not be a problem as long as the relevant comparisons are made. Fig.8B illustrates the protocol we used for the drug experiments. The cells were initially stimulated with 100 mM K^+ in the absence of drug. After the first stimulation cells were flushed with extracellular saline containing the drug. 2 minutes later the cells were stimulated with 100 mM K^+ solution, also containing the drug. Cells were washed several times with extracellular saline and after another 2 minute wait were stimulated a third time with 100 mM K^+, to test for the reversibility of drug action. Drug activity was measured by normalizing second stimulus amplitude to first stimulus amplitude. These normalized amplitudes were compared to normalized amplitudes from control cells without drugs applied. A maximum of three stimulations and one drug was used on a plate of cells.

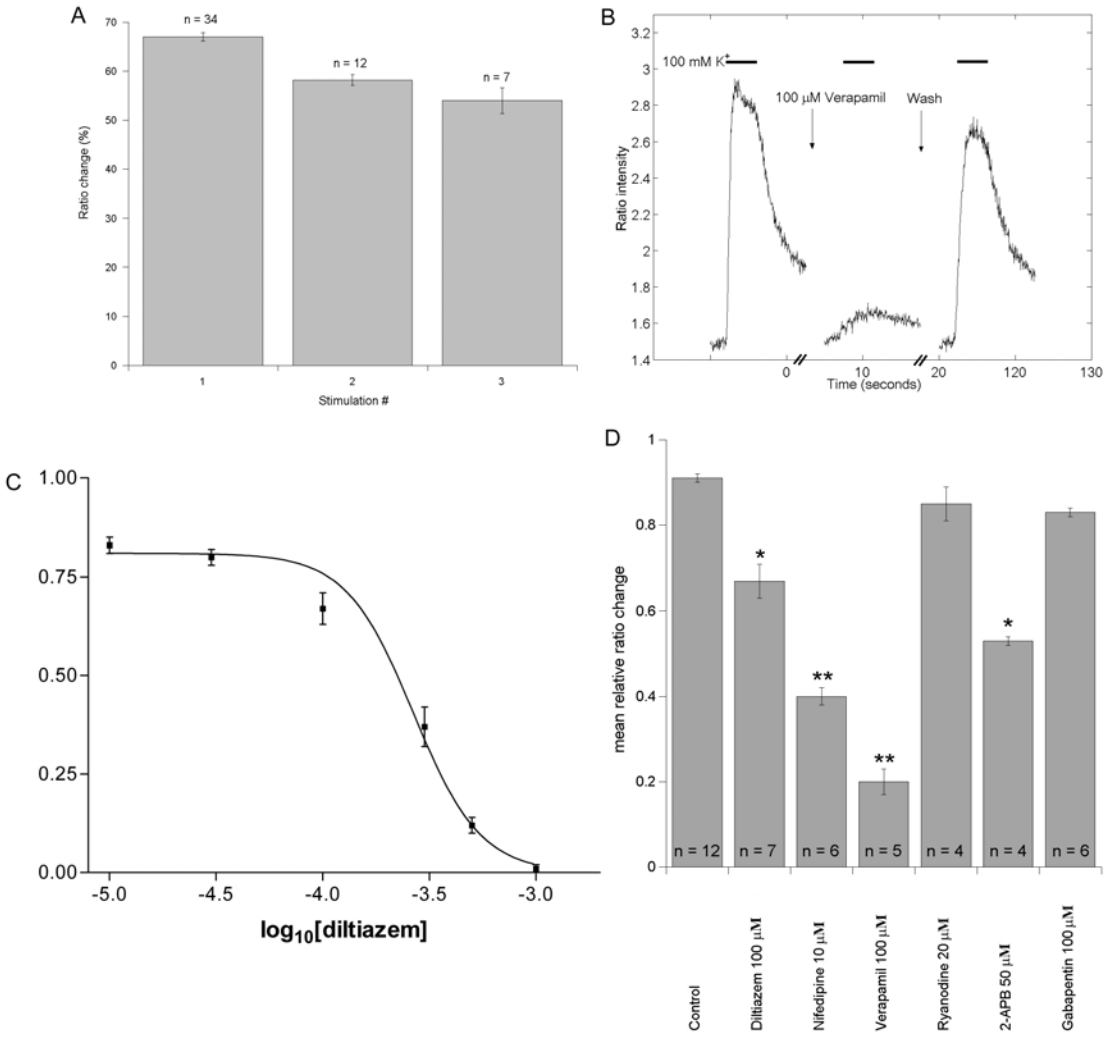

Fig. 8. Wildtype pharmacology

(A) Reproducibility of calcium transient to three successive stimulations with 100 mM K^+ and 2 minutes between stimuli. Varying the depolarizing K^+ concentration or interval between stimuli did not prevent attenuation of transients.

(B) Wild type cultures stimulated with 100 mM K^+ without drug, then in the presence of the L-type calcium antagonist verapamil (100μM) and finally after washout of drug. Cells were incubated approx. 2 minutes with drug before the second depolarization and drug was included in both bath solution and depolarizing K^+ solution. The drug reversibly reduced the amplitude of the calcium transient in response to depolarization.

(C) Dose-dependent reduction of calcium transients with the L-type calcium channel antagonist diltiazem. Cells were subjected to the same experimental protocol as shown in (B) at various drug concentrations. High concentrations of diltiazem (1mM) completely abolished response to depolarization in 38 of 43 cells. The plotted ratio values are normalized to the first depolarization in the absence of drug

(D) Calcium transient amplitude in response to 100 mM K^+ in the presence of L-type channel blockers nifedipine, diltiazem and verapamil; ryanodine receptor antagonist ryanodine; IP_3 receptor antagonist 2-APB and $\alpha_2\delta$ antagonist gabapentin. Wild type control data is from second stimulation of control cells without added drug. Ratio values are normalized to the first stimulation before addition of drug and the error bars indicate standard error of mean. Single asterisk indicates significance $0.01<p<0.05$ and double asterisk indicates high significance ($p\leq0.01$) when compared to control. Statistical analysis was done using a Mann-Whitney rank sum test comparing the control group to each of the tested drugs. p values were corrected for multiple comparisons.

We tested three classes of L type channel blockers, dihydropyridines (i.e. nifedipine) , phenylalkamines (i.e. verapamil) and benzothiazepines (i.e. diltiazem) which bind reversibly to distinct, but overlapping sites in L-type voltage gated channels (Striessnig et al., 1998 and Hockerman et al., 2000).

We aligned the rat brain α_1 L-type calcium channel (rbC-II, genbank accesion number #M67515) with EGL-19 genomic dna. Comparison showed that the drug binding residues for all three classes of drugs were either present in EGL-19 as identical residues (14) or similar residues (4) (fig.9). We therefore expected all three classes of antagonist to block the invertebrate L-type calcium channel EGL-19. In contrast, UNC-2 alignment showed only 6 identical residues, 5 similar and 7 non-similar residues, consistent with the UNC-2 channel being classified as a non-L-type channel (data not shown).

EGL-19 940 IMLVTFMLQFM
Consensus I++VT-+LQFM
rbC-II 1035 IVIVTTLLQFM

EGL-19 1040 VALFFIAFIIVIAFFMMNIFV
Consensus +++FFI-+II+IAFFMMNIFV
rbC-II 1145 ISIFFIIYIIIIAFFMMNIFV

EGL-19 1340 AYPYFISFFMLCSFLVINLF
Consensus A--YFISF+MLC+FL+INLF
rbC-II 1455 AVFYFISFYMLCAFLIINLF

Fig. 9. Alignment of regions involved in drug binding

Schematic showing parts of the aligned rat α_1 L-type calcium channel (Snutch et al., 1991) and EGL-19 amino acid sequence. Underlined residues indicate putative role in dihydropyridine (i.e. nifedipine) sensitivy (Striessnig et al., 1998), **bold** residues are involved in phenylalkamine (i.e. verapamil) sensitivity (Hockerman et al., 2000) and gray colored residues are involved in benzothiazepine (i.e. verapamil) binding (Striessnig et al., 2000). Consensus strand based on identity, similarity (+), or no similarity (-).

Fig.8B shows the reversible antagonist effect of verapamil. 100 μM verapamil reduces the calcium transient amplitude to 20 +-3 % (n = 5) of the initial stimulation, compared to 91% +-1% (n = 12) for the control group.

Fig. 8C shows how diltiazem dose-dependently blocked the calcium transients, yielding an IC_{50} value of approx. 300 μM. Diltiazem also acted reversibly (not shown) and at high concentrations (1mM) completely blocked the calcium transient. Fig.7D summarizes the drug binding experiments. All three classes of L-type calcium channel blockers, diltiazem, nifedipine and verapamil significantly reduced the calcium transients reversibly in response to 100 mM K+ depolarization, indicating a possible role of the EGL-19 L-type channel. The drugs block the calcium currents at concentrations

comparable to vertebrate L-type channels and the potency relationship among the three blockers is retained (Bargas et al., 1994 and Mangano et al., 1991).

We also tested calcium release from intracellular stores. Ryanodine at high concentrations (20μM) can completely and irreversibly block the ryanodine receptor without affecting the calcium homeostasis in cultured sympathetic neurons (Hernández-Cruz et al., 1997). The action is quick and prevents release of calcium from intracellular stores through the ryanodine receptor. Adding 20μM ryanodine in the bath did not significantly change the ratio amplitude (fig.8D).

It was difficult to test for the involvement of inositol-triphosphate receptors (IP_3-receptors) pharmacologically in the calcium transients, since there are no readily available specific IP_3-receptor blockers. Although not ideal, we used the blocker 2-APB for our initial pharmacology screen for possible calcium sources for the transients. Initially, the blocker 2-APB was thought to specifically inhibit IP_3-receptors (Maruyama et al., 1997). A number of later studies have shown that the drug inhibits the store-operated channels (SOCs) that replenish the calcium in intracellular stores and that inhibition of IP_3-receptors depends on the isoform of the receptor. Also, the drug can lead to rapid cytoplasmic acidification (review, Bootman et al., 2002). Application of 2-APB significantly reduced the normalized amplitude to 53 +- 1% (n = 4) hinting at a possible role for intracellular calcium release, although the result should be interpreted with the many caveats in mind.

The drug gabapentin (commercial name Neurontin) is an antiepileptic drug and is also used to treat pain. Gabapentin specifically binds to $\alpha_2\delta$–1 (Gee et al., 1996) and $\alpha_2\delta$-2 but not to $\alpha_2\delta$-3 (Marais et al., 2001). We aligned the three mammalian $\alpha_2\delta$ subunits

and UNC-36 and there was 20.6 %, 19.1% and 20.9% identity to $\alpha_2\delta$–1, $\alpha_2\delta$-2 and $\alpha_2\delta$-3, respectively. We tested gabapentin on the cultured neurons and 100 μM gabapentin did not significantly reduce the normalized calcium transient amplitude, indicating either that gabapentin did not bind to the $\alpha_2\delta$ subunits or there was no effect of binding. Wang et al. (1999) have shown that three regions of $\alpha_2\delta$–1 are important for gabapentin binding and particularly that mutation of the single amino acid R217A completely abolishes gabapentin binding. The corresponding aligned residue in UNC-36 is an asparagine (N246) so based on this alone we would not expect gabapentin to bind to UNC-36. In the two other important regions (AA 515-538 and 582-604 numbered from $\alpha_2\delta$–1) UNC-36 only has 3/6 and 1/5 of the amino acids necessary for gabapentin binding (data not shown).

We also tested the effect of the voltage gated calcium channel agonist bay-K 8644, which binds to vertebrate L-type calcium channels and prolongs the open state of the channel (Schramm et al., 1983 and Bechem and Schramm, 1987). 50 μM Bay-K showed only a small non-significant increase of the normalized amplitude in response to 40 mM K+, and no effect when added to cell culture in the absence of high K+ (data not shown).

Although transient amplitude was progressivel attenuated with the number of stimulations we were able to show an effect of several drugs on calcium influx. In particular, all tested L-type calcium channel blockers significantly reduced the transients indicating a likely role for EGL-19, the only *C.elegans* L-type VGCC. Also, high concentrations of L-type VGCC blockers could block the whole transient indicating that other types of VGCCs did not participate in the calcium influx. From the very beginning

of the project we were also interested in the role of VGCC subunits, especially the $\alpha_2\delta$ subunit UNC-36. Before proceeding to test VGCC mutants and subunit mutants we wanted to know if any of the two $\alpha_2\delta$ subunits were even expressed in the mechanosensory neurons.

$\alpha_2\delta$ expression pattern

Although we could not see any effect of gabapentin on the amplitude of calcium transients we were still interested in determining if UNC-36 had a role in regulating neuronal voltage gated calcium channels. We determined the expression pattern of the two $\alpha_2\delta$ *C.elegans* homologs UNC-36 and T24F1.6 with green fluorescent protein (GFP) to see if the subunits were expressed in the mechanosensory neurons.

We made a construct that drove GFP expression with 1.7 kb of the UNC-36 promoter. The length of the promoter was chosen so that it did not overlap with the adjacent snb-5 gene located 2.0 kb upstream. The 1.7 kb fragment was amplified by PCR from genomic DNA and inserted into a TopoTA vector. The TopoTA plasmid was amplified in competent bacteria, digested with the restriction enzymes BamHI and AgeI and isolated from an 1% agarose gel after electrophoresis. The fragment was ligated into a cut Fire lab vector pPD95.79 containing GFP in an open reading frame. Competent bacteria was transformed with the ligation mixture and antibiotic resistant colonies were selected. The construct was verified with several restriction enzyme digests and all the resulting fragments had the expected size. Plasmid was re-isolated with a midi-prep to get sufficient purity for injection. The plasmid was coinjected with dpy-20(+) gene into the gonad of young dpy-20(e1282ts) hermaphrodites. After a couple of days non-mutant

progeny was isolated from the injected animals and these strains were monitored for transgene propagation to progeny. Several independent transgenic lines were obtained and all showed similar bright GFP expression. GFP was expressed in most neurons and virtually all muscle tissue (body wall muscle and vulva, but only sometimes in the pharynx) (see fig.10). We scored the neurons by Nomarski microscopy and identified expression in the mechanosensory neurons ALM, AVM and PVM (see fig.10D and 10E).

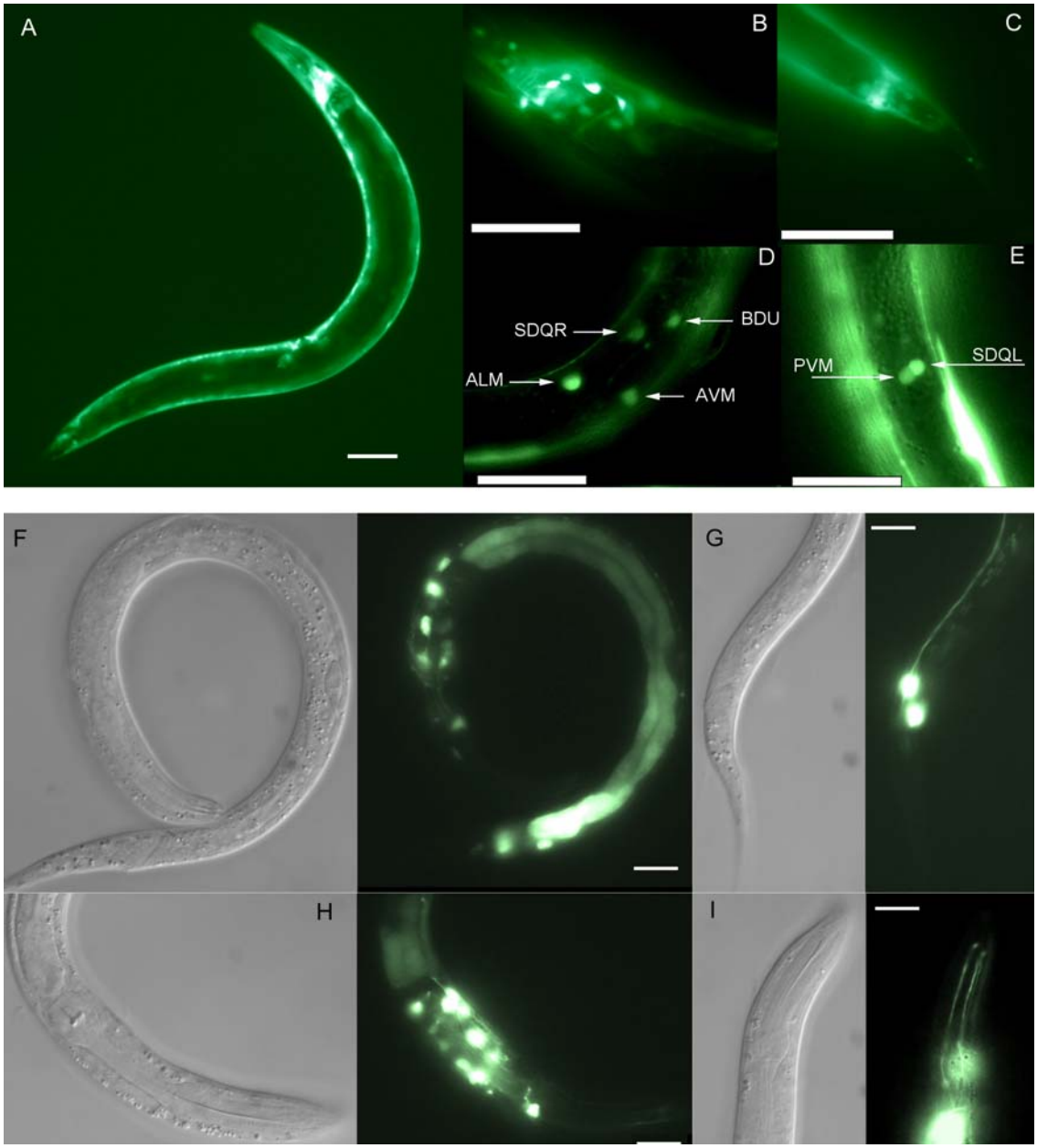

Fig. 10 UNC-36 and T24F1.6 expression patterns. Top UNC-36, bottom T24F1.6

(A) Expression construct pUNC-36::GFP was made by fusing a 1.7 kb upstream region of UNC-36 to GFP. Whole worm image shows expression in both muscle and neurons.
(B) Magnification showing expression in the nerve ring.
(C) Tail expression
(D) Worms in the L2 stage were scored for expression in the mechanosensory neurons by Nomarski. Fluorescence was positively located to AVM, ALM and PVM. Arrows indicate GFP expression in ALM, AVM, BDU and SDQR.
(E) Expression in PVM and SDQL.

(F) Expression construct pT24F1.6::GFP was made by fusing a 1.5 kb upstream region of T24F1.6 to GFP. Expression is seen in a small number of neurons and in the gut. AVM, ALM and PVM were scored by Nomarski and no expression could be seen.
(G) Tail.
(H) Head
(I) Amphid neurons in head.
All scale bars = 50 μm.

We also identified GFP expression in the tail neurons PVQ, PVC, DUC and DVA. PLM, ALN and PHB were probable, but not certain, since these neurons are particularly difficult to identify. In the head GFP was expressed in ASE, AVA, SIBDC, RMDUL, AVA, ASK and a number of unidentified neurons.

Similarly, we made a GFP expression construct with 1.5 kb of the T24F1.6 promoter. This construct was made with a different technique, described by Hobert (2002). The full construct was made by two rounds of PCR, with the first round amplifying the promoter and GFP separately and a second round of PCR, which fused the two fragments together. Two independent transgenic lines were made and expression was seen in a limited number of neurons and in the gut (see fig. 10F-I). Two neurons in the tail and approx. 10 neurons in the head showed GFP expression. At least one of the amphid neurons was clearly labeled with GFP (fig.10I). The neurons were identified again by Nomarski and we could not see any GFP expression in AVM, PVM or ALM. Expression was not seen in SDQR or SDQL, but was present in BDU.

We also constructed UNC-2, UNC-36 and T24F1.6 full length protein GFP fusions in the hope of determining the subcellular localization of these proteins. The subcellular localization could give indications of possible functional roles and interactions with subunits. It would for example be interesting to see if UNC-2 localizes to the synapse and if UNC-36 co-localizes with UNC-2, EGL-19 or both. Unfortunately,

we only succeeded in obtaining transgenic animals with the UNC-2 and the T24F1.6 constructs. Of these, only the T24F1.6::GFP construct was fluorescent. Transgenic animals were obtained, but the expression did not localize to the membrane, although the expression pattern was similar to the smaller promoter fusion construct (data not shown). We believe there are several possible causes for the trouble associated with the full length constructs. The additional length (approximately 7kb for the $\alpha_2\delta$ subunits and 14kb for UNC-2) reduced the yield of the constructs made by pcr fusion and made an additional cleaning step impossible. Also, the error in PCR increases with increasing length and we did not have the finished constructs sequenced for verification, so there could possibly be errors in the coding regions. The lack of membrane association of the T24F1.6 construct is perhaps not surprising, since there is only a small 3-4 amino acid intracellular domain in $\alpha_2\delta$ to attach the GFP to and this has possibly corrupted the normal membrane insertion.

The expression data gave us reason to believe that UNC-36 was the only $\alpha_2\delta$ subunit expressed in the mechanosensory neurons and that T24F1.6 would not be able to substitute for the lack of UNC-36 in *unc-36* mutants. There are many caveats for assessing the gene expression with GFP expression constructs (A. Fire, documentation for expression vectors) and in the next section we show that data from *unc-36* mutants also indicate a functional role for UNC-36 in cultured mechanosensory neurons.

EGL-19 and UNC-36 loss of function mutations decrease amplitude of calcium transients

There are a number of *C.elegans* strains readily available, which have mutations in genes involved in calcium flux and homeostasis. We primarily focused on the voltage gated calcium channel mutants *egl-19(ad1006)*, *unc-2(lj1)* and the $\alpha_2\delta$ subunit loss of function mutant *unc-36(e251)*.

EGL-19 null mutants are lethal but several loss of function mutants have been characterized behaviorally (Lee et al., 1997). *egl-19(ad1006)* belong to the flaccid class of loss of function mutants with feeble pharyngeal contraction, defective egg-laying and slow movement. *unc-2(lj1)* has a large deletion, eliminating most of the third and fourth membrane domain and is a probable null mutant (Tam et al., 2000). *unc-36(e251)* is also a loss of function allele and worms carrying the mutation are very slow, thin and almost paralyzed (*C.elegans* II, 1997). Also, the worms do not respond to taps on the lid of the petri dish, which causes wildtype worms to reverse. The role of *unc-36(e251)* and *egl-19(ad1006)* in calcium flux was previously studied in the pharyngeal muscles during pumping (Kerr et al., 2000). We examined the effect of *egl-19(ad1006)*, *unc-36(e251)* and *unc-2(lj1)* on transient amplitude in response to depolarization. Representative averaged traces of the mutant strains are shown in fig.11A.Each trace corresponds to one experiment with several neurons. For each allele the traces were averaged to bring out the essential features and normalized to a common baseline for comparison. *egl-19(ad1006)* and *unc-36(e251)* were clearly distinguishable from wild type traces. *unc-2(lj1)* traces were indistinguishable from wild type traces (trace not shown).

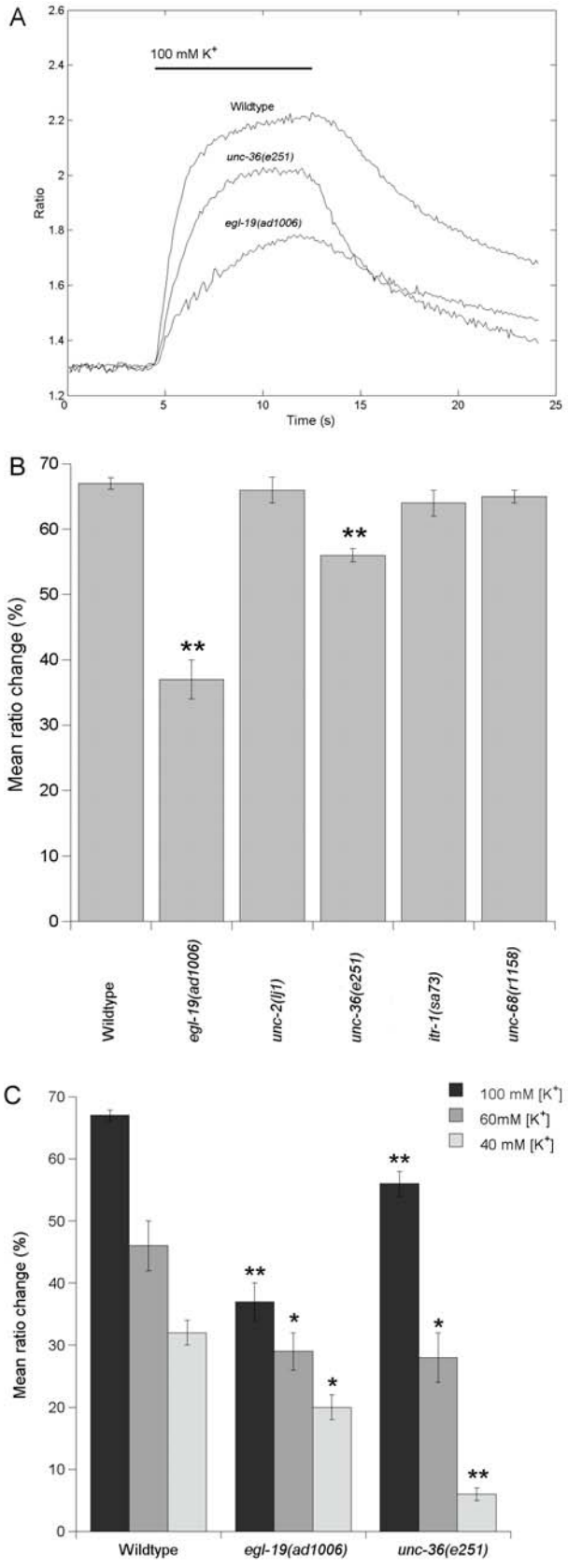
A
100 mM K+
Wildtype
unc-36(e251)
egl-19(ad1006)
Ratio
Time (s)
B
Mean ratio change (%)
**
**
Wildtype
egl-19(ad1006)
unc-2(lj1)
unc-36(e251)
itr-1(sa73)
unc-68(r1158)
C
100 mM [K+]
60mM [K+]
40 mM [K+]
Mean ratio change (%)
**
*
*
**
*
**
Wildtype
egl-19(ad1006)
unc-36(e251)

Fig.11. Mutant response to depolarization

(A) Representative averaged traces from wildtype, *unc-36(e251)* and *egl-19(ad1006)* responding to depolarization with 100 mM K^+. Each trace is an average of one experiment with a number of neurons (wildtype 11 cells, *unc-36(e251)* 8 cells, *egl-19(ad1006)* 15 cells). The averaged traces have been normalized to a common pre stimulation baseline for visual comparison. *unc-36(e251)* and *egl-19(ad1006)* both show a significant decrease in amplitude and a qualitative change in shape.

(B) Wild type and mutant response to100 mM K^+ depolarization. The plotted value for each mutant strain is the average response to the initial depolarization of the cells. Each plate of cells is treated as one independent trial. The individual cells and the mean ratio of all the cells on a plate is used. For wildtype this corresponds to 34 independent trials with a total of 307 neurons. *egl-19(ad1006)* and *unc-36(e251)* show a highly significant decreases in ratio amplitude compared to wildtype.

(C) Detailed comparison of wildtype, *egl-19(ad1006)* and *unc-36(e251)* at different depolarizations. At all the tested K^+ concentrations there is a significant or highly significant reduction in ratio amplitude. At lower K^+ concentrations there were a larger number of non-responsive cells. All cells were subsequently depolarized with 100 mM K^+ to ensure the overall health of the cells. Only cells responsive to a subsequent depolarization with 100 mM K^+ were used.

All values are mean ± standard error of mean. Statistical analysis was done using a Mann-Whitney rank sum test compensated for multiple comparisons. Single asterisk indicates significance ($0.01 < p < 0.05$) and double asterisk indicate high significance ($p \leq 0.01$) compared to wildtype control.

Analysis of the mean ratio increase in response to 100 mM K^+ showed a statistically significant reduction in amplitude for *egl-19(ad1006)* and *unc-36(e251)* to 37 +-3 (n = 8) and 56 +- 2 % (n = 31) respectively, compared to 67 +- 1 % (n = 34) for wildtype controls (see fig.11B).The *unc-2(lj1)* allele showed no significant reduction in amplitude 66 +- 1 % (n = 41).

The role of intracellular calcium stores was tested with the ryanodine receptor putative null mutant *unc-68(r1158)* (Maryon et al., 1996) and the weak loss of function inositol triphosphate mutant *itr-1(sa73)* allele (Dal Santo et al., 1999). UNC-68 is the only ryanodine receptor and ITR-1 is the only IP3 receptors in *C.elegans* and both have been associated with specific phenotypes in muscle (Maryon et al., 1996 and Dal Santo, 1999). Experiments with *unc-68(r1158)* and *itr-1(sa73)* showed no statistically significant reduction in mean ratio amplitude nor any apparent change in transient shape (fig. 11B).

Cultured *unc-36(e251)* and *egl-19(ad1006)* neurons were also stimulated with 40mM K^+ and 60mM K^+. The reduction in ratio amplitude was significant and consistent for all three different depolarizations for both strains, with *unc-36(e251)* showing the largest dependence on K^+ concentration (see fig.11C).

itr-1(sa73) was also tested at 40 mM K^+ and 60 mM K^+ to further investigate the pharmacological result with the IP_3 receptor antagonist 2-APB. At 60 mM K^+ stimulation *itr-1(sa73)* is indistinguishable from wildtype and at 40 mM K^+ the ratio amplitude is slightly higher than wild type transients (see appendix 1).

These results on mutant strains complement the pharmacological and expression pattern data. *egl-19(ad1006)* loss of function mutants show consistently reduced calcium transient amplitudes in good agreement with the effect of L-type calcium channel blockers. The surprisingly large effect of *unc-36(e251)* confirms the expression of UNC-36 in the mechanosensory neurons. This result would also seem to strengthen the claim that T24F1.6 is not able to substitute for UNC-36 in the mechanosensory neurons – possibly because the two subunits have different molecular interaction partners or simply because T24F1.6 is not expressed in these neurons.

Conclusion/Discussion

The pharmacological and genetic data suggests a role for the L-type calcium channel EGL-19 in regulating calcium influx into cultured mechanosensory neurons in response to depolarization. Alignment of EGL-19 and a vertebrate L-type calcium channel showed highly conserved drug binding regions for dihydropyridines, benzothiazepines and phenylalkamines. These L-type channel blockers can completely block the transients. Also, we cannot detect transients in the absence of extracellular calcium. From this we conclude that [Ca^{2+}] entering the cell through the L-type VGCC EGL-19 is necessary for generating transients. The reduced transient amplitude in *egl-19(ad1006)* loss of function mutants further supports this. It should be noted that the recording protocol used favors detecting calcium influx through L-type calcium channels because of the long depolarization and because we have focused the imaging on the cell body. Non-L type channels, such as UNC-2, would be expected to inactivate quickly and therefore not contribute as much to the calcium transient as the slowly inactivating L-type channel. If this were a significant effect, we would expect to see an initial rapid calcium transient independent of the pharmacologically blocked L-type channel. Inspection failed to show such an initial transient even in the presence of high concentrations of dihydropyridines, which are known to selectively block L-type VGCCs.

The involvement of EGL-19 in generating the transients does not rule out an additional role for intracellular calcium release through ryanodine receptors or IP_3 receptors. There is only one ryanodine receptor, UNC-68, in the *C.elegans* genome and results with ryanodine and the putative null mutant *unc-68(r1158)* do not indicate a role for the ryanodine receptor in generating transients. The results with the IP_3 receptor are more ambiguous, with an effect of 2-APB but variable effects of the *itr-1(sa73)* mutation.

The genetic data also suggests a role for the $\alpha_2\delta$ subunit UNC-36 in cultured mechanosensory neurons. In contrast with earlier results in the pharyngeal muscle using cameleons (Kerr et al. 2000) the UNC-36 mutation has a negative effect on calcium flux. Kerr et al. (2000) proposed that UNC-36 possibly acts as a direct negative regulator of voltage gated calcium channels in *C.elegans* muscle. Alternatively, UNC-36 could be functionally important for synaptic transmission from inhibitory neurons to the pharyngeal muscles and presumably not essential for voltage gated calcium channel activation in the pharynx. The latter hypothesis has the advantage of requiring only a single function for UNC-36, namely to enhance calcium flux in neurons. Characterization of the non-L type calcium channel UNC-2 would also seem to favor the second explanation. Schafer et al. (1996) studied the effect of *unc-2* and *unc-36* loss of function mutations on serotonin sensitivity. It was concluded that UNC-36 and UNC-2 most likely interact and are involved in the release of neurotransmitter at the cholinergic VC neurons. Also, acetylcholine acted as an inhibitory neuromodulator of vulval muscle serotonin sensitivity. Since Kerr et al. (2000) directly induced pharyngeal pumping with exogenous serotonin, lower acetylcholine release in the unc-36 background could lead to increased serotonin sensitivity and higher calcium flux. It should be noted, that although *unc-2*, *unc-36* and the double mutant phenotypes were reported to be essentially identical, Schafer et al.(1996) also noted subtle differences indicating distinct roles for UNC-2 and UNC-36 in muscle and neurons. *unc-2* males are able to mate, in contrast to *unc-36* males, which led to speculation of a separate calcium channel, other than UNC-2, associated with UNC-36. Conversely, *unc-2* shows neuronal migration defects, but not *unc-36*, indicating a functional UNC-2 calcium channel without UNC-36.

Another line of evidence that suggests a role for UNC-36 and UNC-2 in neurotransmitter release is that *unc-36* and *unc-2* mutants show resistance to the acetylcholinesterase inhibitors aldicarb and trichlorfon (Nguyen et al, 1995). These inhibitors increase the levels of acetylcholine (ACh) leading to hypercontraction. Other resistant mutants have specific defects in neurotransmitter release, ACh synthesis or ACh responsiveness (Miller et al., 1996). It is not known if the cultured neurons form functional synapses and if the synaptic proteins localize correctly. If UNC-2 preferentially locates to the synapse and is involved in neurotransmitter release it could explain why we do not see a significant effect of the *unc-2(lj1)* mutation in the cell body. Unfortunately, the full length UNC-2::GFP construct, which could have at least partially answered this question, was not functional.

The pharmacological and genetic data indicates that the recorded calcium transient is almost exclusively dependent on the flux through EGL-19 channels. The *unc-36(e251)* loss of function mutant significantly decreases the calcium transient amplitude and we interpret this as an indication towards an interaction between UNC-36 and EGL-19 in neurons. These newer results are more consistent with the electrophysiological data available from vertebrate studies (Letts et al., 1998 and Brodbeck et al., 2002). Also, attempts to reproduce the previous results from pharyngeal muscle with UNC-36 gave variable results depending on experimental conditions and the experimenter. This sensitivity to external factors is more consistent with a role for UNC-36 in neuronal regulation of pharyngeal activity, than with a direct role in pharyngeal muscle contraction.

Further studies using other UNC-36 and EGL-19 alleles would be desirable to rule out interference from the genetic background. Also, co-localization studies with GFP tagged full length proteins would be helpful to study the possible interaction in greater detail.

The studies have furthermore shown that three subclasses of DHPs (Nifedipine, Diltiazem and Verapamil) also block invertebrate calcium channel flux at similar concentrations to vertebrate channels. Although the impermeant cuticle limits the usefulness of *C.elegans* to search for novel pharmacological compounds it further validates the use of *C.elegans* in determining molecular targets of pharmacological agents.

The cultured cells made it possible to calibrate the cameleon sensor *in situ*. The sensitivity of the cameleon sensor was not drastically altered compared to the *in vitro* characterization of the yc2.1 version previously published (Miyawaki et al, 1999). The calibration also estimates the intracellular free calcium in cultured neurons to 200 nM, which is in good correspondence with the accepted value for vertebrate neurons and muscle (Hille, 1992). To our knowledge, this is the first measurement of intracellular calcium concentration in *C.elegans* neurons.

We have shown that the combined use of genetically encoded calcium indicators and primary culturing techniques successfully can be used to study basic biophysical mechanisms in *C.elegans* neurons. The techniques complement the large knowledge and availability of genes with known mutations.

Materials and Methods

Strain handling:

Nematode strains were maintained at room temperature on standard nematode growth medium (NGM) seeded with *Escherichia coli* strain OP50 as food source. In order to collect eggs for primary cultures nematodes were grown in larger scale at room temperature on enriched peptone plates seeded with *Escherichia coli* strain NA22. All cameleon experiments were done on the integrated line bzIs18, expressing yellow cameleon version 2.12 (yc2.12) under the control of the promoter *mec-4*.

***C.elegans* primary cultures**:

C. elegans primary cultures were prepared from synchronized worms as described by Christensen et al. (2001). Briefly, young gravid adults were treated with a 0.5 M NaOH and 1% NaOCL solution for 5 minutes to release eggs. After several washes with egg buffer (118 mM NaCl, 48 mM KCl, 2 mM CaCl2, 2 mM MgCl2 and 25 mM HEPES, pH 7.3, 340 mOsm), eggs were isolated from adult carcasses by centrifugation in a 30% sucrose gradient. The isolated eggs were resuspended in a small volume of sterile water and added to 0.5 mL egg buffer containing nominally 1U/mL chitinase (Sigma Chemical, St. Louise, MO) to digest the eggshell. Eggs were digested 15-20 min on a turning rack and washed once with culturing medium L-15 (Life Technologies, Grand Island, NY) containing 10% fetal bovine serum (Life Technologies), 50 U/ml penicillin, 50 ug/ml streptomycin and osmolarity of 340 mOsm. Eggs were dissociated by pipetting the solution up and down in an Eppendorf tube with a 1 ml pipettor. When a satisfactory degree of dissociation had been achieved the cells were pelleted and resuspended in fresh

L-15 solution. Single cells were isolated from undissociated eggs and clumps of cells by filtration through a 5 μm Durapore filter (Millipore, Bedford, MA). The single dissociated cells were washed once in L-15 and plated at a concentration of $2.5*10^4$ cells/μL on UV sterilized 12 mm acid washed cover glass (Fisher Scientific, Pittsburgh, PA) coated with 1 mg/ml peanut lectin (Sigma). Cells were cultured in 24 well Costar culture plates (Corning Inc., Corning, NY) and left for two hours on cover glass to adhere before filling the well with L-15 growth medium. Cells were grown in plastic boxes containing wet tissues in a 25°C incubator. All culturing was carried out on a lab bench using sterile techniques.

Optical Imaging:

2-3 day old cells were placed in a RC-26 GLP open recording chamber (Warner Instrument Corp., Hamden, CT) and attached to the bottom of the well with vacuum grease. Cells were perfused with an extracellular saline solution (145 mM NaCl, 5 mM KCl, 2 mM $CaCl_2$, 1 mM $MgCl_2$, 10 mM HEPES, 10 mM d-Glucose, pH 7.2 and 340 mOsm) to remove culture medium and non-adherent cells. Optical recordings were done on a Zeiss Axioscop 2 upright compound microscope with a Hamamatsu Orca ER II CCD camera, a Hamamatsu W-view emission image splitter and a Uniblitz Shutter (Vincent Associates). Recordings were done on a 1200 MHz Athlon (Advanced Micro Devices) computer with the program MetaVue 4.6 (Universal Imaging Corp., Downingtown, PA) running Windows 98 (Microsoft). Images were acquired at 10 Hz (100ms exposure time) with 4x4 binning, using a 63x Zeiss Achroplan water immersion objective. Filter/dichroic pairs were: excitation, 420/40; excitation dichroic 455; CFP

emission, 480/30; emission dichroic 505; YFP emission, 535/30 (Chroma). Healthy looking cameleon expressing neurons were located by eye under minimal fluorescence to minimize photo bleaching. Before starting the recording cells were perfused with extracellular solution for 5 s to stabilize the solution level in the recording chamber. The recording protocol consisted of 3-5 s extracellular saline perfusion, 8 s high K^+ solution and 12-14 s extracellular saline. The high K^+ solution was a modified version of the extracellular saline solution with variable amounts of KCl substituted for NaCl. The solutions were delivered with a gravity feed perfusion system, with 6 solution tubes reaching a manifold (Warner Instruments) and one tube entering the recording chamber with a flow rate of approximately 0.5 ml/s.

Stacks of images were acquired with MetaVue (Universal Imaging) and saved to a computer hard drive. A custom written Java-based program (Kerr, 2002) was used to define regions of interest. The program automatically tracked these regions and reported the total CFP and YFP intensity for each frame.

The separation of the YFP and CFP emission with filters was not perfect. We measured the crosstalk between the two channels with purified CFP or YFP protein. The correction parameters for crosstalk between the CFP and the YFP channel was measured to be: YFP emission crosstalk Ca/Da = 0.01, CFP emission crosstalk Cd/Dd = 0.60, where Dd and Da are the detector quantum efficiencies through the correct channel and Cd and Ca are the detector quantum efficiencies through the wrong channel. Given the relative small size of Ca/Da only the Cd/Dd crosstalk was corrected for, effectively subtracting 60% of the CFP intensity from the YFP intensity.

Ratios were further analyzed and plotted for visual inspection using custom written analysis scripts in MATLAB R12 (The Mathworks). The ratio trace was low-pass filtered with a gaussian blur of the form $e^{-(x/\sigma)^2}$. Event were detected as N of M successive frames displaying an increase corresponding to a slope of at least s. The parameters N, M and s were varied slightly between different experiments to give satisfactory event detection as judged by eye. The blur was kept constant at $\sigma = 8$ for K^+ induced transients to prevent skewing of data.

All drugs were purchased from Sigma (Sigma Chemical, St. Louise, MO) except 2-APB which was ordered from Calbiochem (Calbiochem-Novabiochem Corp., La Jolla, CA). Solutions were made from at least 500x stock solutions in either DMSO or dH_20.

Cameleon calibration:

Calibration of the cameleon yc2.12 was performed on cultured bzIs18 worms. We mimicked a protocol from Thomas et al. (2000), which included the mitochondrial inhibitor Rotenone (10 μM) and the glycolytic inhibitor 2-deoxy-D-glucose (1.8 mM) in the calcium buffer to deplete the cells of ATP and inhibit Ca ATPases. This proved necessary to get stable calcium ratios at low calcium concentrations.

The cultured cells were transferred from the culture medium to nominally calcium free extracellular bath solution (0 mM Ca^{2+}, 0 mM EGTA. pH 7.2, 340 mOsm) to remove extracellular calcium contaminants. The cells were transferred from the bath solution to a calcium buffered solution including Rotenone (10 μM), 2-deoxy-D-Glucose (1.8 mM) and the non-fluorescent calcium ionophore Br-A23187 (10 μM). The osmolarity was adjusted to 340 mOsm with sucrose. Cultured cells were allowed to equilibrate in dark

for 30 min in buffer and then transferred to new buffer solution in recording chamber. Cells were ratio imaged continuously for 15 min – 5 min in calcium buffer, 5 min in nominally free calcium buffer (0 mM Ca^{2+}, 5 mM EGTA. pH 7.2, 340 mOsm) and 5 min in high calcium (10 mM Ca^{2+}, pH 7.2, 340 mOsm). Cells were flushed with extracellular 0 mM Ca^{2+} solution between all solution changes to avoid the large pH shift associated with calcium binding to EGTA. Ratios were extracted as described in the optical imaging section. Calcium buffers with free calcium in the range from 10nM to 40 μM and pH in the range from 6.8 to 8.0 were purchased from World Precision Instruments (Sarasota, FL). The calibration data was fit to a two site competitive binding model with distinct affinities for the two sites in the program GraphPad Prism (GraphPad Software Inc., San Diego, CA).

Baseline calcium concentration was measured by imaging cultured neurons for 3 minutes in standard bath solution, before determining R_{max} and R_{min}. R_{max} was determined by shifting the bath solution to a solution containing 5mM EGTA, 10 μM Br-A23187 and 10 μM ionomycin to improve access to cells, 10 μM rotenone and 1.8 mM 2-deoxy-D-glucose. Cells were washed with calcium free extracellular solution and R_{max} was determined by incubating the cells with 10 mM $CaCl_2$, ionophores and metabolic blockers.

Molecular biology:

A UNC-36 promoter GFP fusion was constructed by amplifying a 1.7 kb promoter region by PCR from genomic dna with the primers 5'-GGATCCGATTTGTTTGTTGCGCG CCGG–3' and 5'-

ACCGGTGATGAACCACTCGCTTTCTCG–3’ corresponding to 1687 bps upstream of the translation start site. The second primer overlaps with the translation start and has a deliberate missense mutation to change the start codon. The pcr product was inserted into a topo TA vector. BamH I and Age I restriction enzymes were used to circularize the fire lab vector pPD95.79 and to cut out the topo-TA-PCR product. PCR product and pPD95.79 were ligated and amplified in competent bacteria. The purified promoter GFP construct was coinjected with dpy-20(+) gene into *dpy-20(e1282ts)* following the protocol in Mello and Fire (1995) to obtain strains propagating the plasmid as an extrachromosomal array.

The T24F1.6 full length and promoter GFP fusions were prepared by PCR fusion, following the protocol of Hobert (2002). T24F1.6 full length fusion was amplified with upstream primers 5’ – GGATCCGAAATTCTATTCATTCTTCTCATCTCAAAACCC – 3’ and 5’ – CCCTCAATTTGATCCCTCTCCTC – 3’, corresponding to 1385 and 1354 bp upstream of the translation start. The PCR overlap primer was 5’-AGTCGACCTGCAGGCATGCAAGCTGAATATCCGAAAAGTTGATATGAGAATGAGC–3’ and the two GFP primers 5’ – AAGGGCCCGTACGGCCGACTAGTAGG – 3’ and 5’ – GGAAACAGTTATGTTTGGTATATTGGG – 3’.

The T24F1.6 promoter GFP fusion was amplified with the same primers as the full length fusion except for the overlap primer, where two sets of primers were used : 5’- CTAGAGTCGACCTGCAAGGCGGTCATTGTTGAAGTATTTCG – 3’ and 5’ – CGAAATACTTCAACAATGACCGCCTTGCAGGTCGACTCTAG – 3’.
Full length and promoter T24F1.6 dna were amplified from genomic dna and the GFP from fire lab vector pPD95.75 by pcr with the Expand Long Template PCR System

(Roche). Gel extracted dna was coinjected with lin-15(+) gene into *lin-15(n765ts)* and lines stably transmitting the injected dna were obtained.

Statistics

Statistical analysis was done using the non-parametric Mann-Whitney rank sum test. Initial analysis of the individual data points showed that the values were non-normally distributed. This could be due to several factors – noticeably non-responsive cells, especially at lower K^+ concentrations, and an upper limit to the ratio change limited by the maximal ratio change of the cameleon sensor. Each plate with several neurons was treated as one independent experiment and the mean ratio change of all the cells used. Statistical values were corrected for multiple corrections using the Bonferroni correction.

Acknowledgements

I would especially like to thank Prof. Schafer for having me in his lab at University of California, San Diego and for giving me opportunities to learn new techniques with study trips to Oregon and Tennessee. His financial and scientific support made it possible to extend my stay at UCSD.

Thanks to Dr. Rex Kerr for all his skill and patience in training me and helping in the lab. His technical expertise as well as helpful suggestions and discussions of experiments was invaluable for this project. Thanks to Dr. Hiroshi Suzuki for making the original cameleon construct used for the calcium imaging experiments and for help with my initial molecular biology constructs. Thanks to Dr. Massimo Hilliard for help with the overlap PCR technique and help in scoring the neuronal identity of neurons expressing GFP in the expression studies. Thanks to Katie Kindt for help with scoring the touch neurons in the head.

I would like to thank Dr. A. Fire for GFP expression vectors and to the Caenorhabditis Genetics Center for supplying strains. I would like to thank Prof. Kevin Strange at Vanderbilt University and Dr. Michael Christensen for teaching me the primary culture technique before publication of the technique. Thanks to the Tsien lab for providing purified yc2.1 protein and technical assistance from Varda Lev-Ram.

Thanks to my Danish speciale advisor Dr. Stig Steenstrup, for help during the speciale project but also for initial help in organizing the exchange stay at UCSD. Also many thanks to Dr. S.P-Olesen for encouragement, help and guidance.

I would like to thank University of Copenhagen, Psykiatrisk Forskningsfond, Novo Nordisk and Howard Hughes Foundation for financial support.

Appendix 1

Tabulated experimental results

Wild type excitability (Is18)

K conc	Mean ratio change (%)	SEM	Independent trials	Cells
20	3.2	1.5	3	31
40	32	7	12	102
60	51	4	6	46
80	61	3	6	29
100 #1	67	0.9	34	307
100 #2	58	1.1	12	98
100 #3	54	2.6	7	60

#1, #2, #3 indicate first, second and third successive stimulation

Diltiazem dose-response

Diltiazem concentration (μM)	Mean normalized ratio change (%)	SEM	Independent Trials	Cells
10	0.83	0.02	3	25
30	0.80	0.02	2	20
100	0.67	0.04	7	67
300	0.37	0.05	3	35
500	0.12	0.01	2	27
1000	0.01	0.01	6	43

Ratio changes are normalized to preceding stimulus without drug.

Pharmacology

Drug (concentration)	Mean normalized Ratio change (%)	SEM	Independent trial	Cells	p-value
Control (no drug)	0.91	0.01	12	98	-
Diltiazem (300μM)	0.37	0.05	3	35	0.015
Diltiazem (100 μM)	0.67	0.04	7	67	0.009
Nifedipine (10 μM)	0.40	0.02	6	51	0.005
Verapamil (100 μM)	0.20	0.03	5	59	0.01
Ryanodine (20 μM)	0.85	0.04	4	33	0.43
2-APB (50 μM)	0.53	0.01	4	35	0.03
Gabapentin (100 μM)	0.83	0.01	6	51	0.12

p values calculated with Mann-Whitney rank sum test. p-values are corrected for multiple comparisons in this table.

Mutant strains

Depolarization with 100 mM K^+:

Strain	Mean ratio change (%)	SEM	Independent trials	Cells	p-value
Wild type (Is18)	67	0.9	34	307	-
egl-19(ad1006)	37	3	8	88	$7*10^{-5}$
unc-36(e251)	56	2	31	312	$2*10^{-6}$
unc-2(lj1)	66	1.4	41		0.6
itr-1(sa73)	64	1.9	13	116	0.2
unc-68(r1158)	65	1.0	21	178	0.4

p values calculated with Mann-Whitney rank sum test. p-values corrected for multiple comparisons in this table.

Wild type

K concentration (mM)	Mean ratio change (%)	SEM	Independent trials	Cells
100	67	0.9	34	307
60	46	4	11	82
40	32	1.9	12	102

unc-36(e251)

K concentration (mM)	Mean ratio change (%)	SEM	Independent trials	Cells	p-value
100	56	1.5	31	312	$2*10^{-6}$
60	28	4	15	115	0.026
40	5.8	1.4	15	110	$3*10^{-5}$

egl-19(ad1006)

K concentration (mM)	Mean ratio change (%)	SEM	Independent Trials	Cells	p-value
100	37	3	8	88	$7*10^{-5}$
60	29	3	8	81	0.02
40	20	2	8	78	0.0098

p values calculated with Mann-Whitney rank sum test. p-values corrected for multiple comparisons in this table.

Non-responsive cells wild-type

100 mM K+: 3/307 cells
60 mM K+: 1/47 (when sorted for cells responsive to 100 mM K+)
40 mM K+ 13/102 (when sorted for cells responsive to 100 mM K+)

Cameleon calibration data

Calcium concentration	DeltaR/Rmax	SEM	Cells
10 nM	0.00	0.01	5
40 nM	0.02	0.01	5
100 nM	0.21	0.04	6
250 nM	0.25	0.03	7
500 nM	0.41	0.04	4
750 nM	0.47	0.07	5
1 μM	0.50	0.01	5
4 μM	0.76	0.01	6
10 μM*	0.71	0.05	4
40 μM	0.93	0.03	4
100 μM	0.96	0.04	5

* I repeated the 10 μM experiment, because it looks like it is "off". In the second experiment the baseline was not stable, so I have not included the second result. The second result looked like it was even lower than 0.71.

References:

Bangalore, R., Mehrke,G., Gingrich, K., Hofmann, F., Kass, R.S. (1996). Influence of L-type Ca channel alpha 2/delta-subunit on ionic and gating current in transiently transfected HEK 293 cells. Am. J. Physiol. 270: H1521-8.

Bargas J, Howe A, Eberwine J, Cao Y, Surmeier DJ. (1994) Cellular and molecular characterization of Ca2+ currents in acutely isolated, adult rat neostriatal neurons. J Neurosci.14:6667-86

Bargmann, C.I.. (1998). Neurobiology of the Caenorhabditis elegans Genome. Science 282: 2028-2033.

Bechem, M. and Schramm, M. (1987) Calcium-agonists. J. Mol Cell Cardiol. 19: 63-75.

Bootman, M.D., Collins, T.J., Mackenzie, L., Roderick, H.L., Berridge, M.J. and Peppiatt, C. (2002). 2-Aminoethoxydiphenyl borate (2-APB) is a reliable blocker of store-operated Ca2+ entry but an inconsistent inhibitor of InsP3-induced Ca2+ release. FASEB 16: 1145-1150.

Brodbeck, J., Davies, A., Courtney, J.M., Meir, A., Balaguero, N., Canti, C., Moss, F.J., Page, K.M., Pratt, W.S., Hunt, S.P., Barclay, J., Rees, M. and Dolphin, A.C. (2002). The ducky mutation in Cacna2d2 results in altered Purkinje cell morphology and is associated

with the expression of a truncated alpha 2 delta-2 protein with abnormal function. J Biol Chem 277:7684-93.

Catterall, W.A.. (2000). Structure and regulation of voltage-gated Ca^{2+} channels. Annu. Rev. Cell Dev. Biol. 16: 521-55.

C. elegans II. Riddle, Donald L.; Blumenthal, Thomas; Meyer, Barbara J.; Priess, James R., editors. Plainview (NY): Cold Spring Harbor Laboratory Press; c1997.

Chavis, P., Fagni, L., Lansman, J.B. and Bockaert, J. (1996). Functional coupling between ryanodine receptors and L-type calcium channels in neurons. Nature 382: 719-722.

Christensen, M., Estevez, A., Yin, X., Fox, R., Morrison, R., McDonnell, M., Gleason, C., Miller, D.M. 3rd and Strange, K.. (2002). A primary culture system for functional analysis of *C. elegans* neurons and muscle cells. Neuron 33: 503-514.

Dal Santo P, Logan MA, Chisholm AD, Jorgensen EM. (1999). The inositol trisphosphate receptor regulates a 50-second behavioral rhythm in C. elegans. Cell 98: 757-67.

Franks, C.J., Pemberton, D., Vinogradova, I., Cook, A., Walker, R.J., Holden-Dye, L. (2002). Ionic basis of the resting membrane potential and action potential in the pharyngeal muscle of Caenorhabditis elegans. J Neurophys. 87: 954-61.

Gee, N.S., Brown, J.P., Dissanayake, V.U., Offord, J., Thurlow, R., Woodruff, G.N. (1996). The novel anticonvulsant drug, gabapentin (Neurontin), binds to the alpha2delta subunit of a calcium channel. J Biol Chem 271: 5768-76.

Goodman, M.B., Hall, D.H., Avery, L. and Lockery, S.R. (1998). Active Currents Regulate Sensitivity and Dynamic Range in *C.elegans* Neurons. Neuron 20:763-772.

Hernández-Cruz, A., Escobar, A.L., and Jiménez, N. (1997). Ca^{2+}-induced Ca^{2+} Release Phenomena in Mammalian Sympathetic Neurons Are Critically Dependent on the Rate of Rise of Trigger Ca^{2+}. J. Gen. Phys. 109:147-167.

Hille, B., Ionic Channels of Excitable Membranes, Sinauer, Sunderland, MA, 3rd edition, 2001.

Hobert, O. (2002) PCR fusion-based approach to create reporter gene constructs for expression analysis in transgenic *C. elegans*. Biotechniques 32: 728-730.

Hockerman, G.H., Dilmac, N., Scheuer, T. and Catterall, W.A. (2000). Molecular Determinants of Diltiazem Block in Domains IIIS6 and IVS6 of L-type Ca^{2+} channels. Molecular Pharmacology 58: 1264-1270.

Jay, S.D., Sharp, A.H., Kahl, S.D., Vedvick, T.S., Harpold, M.M. and Campbell, K.P. (1991). Structural characterization of the dihydropyridine-sensitive calcium channel alpha 2-subunit and the associated delta peptides. J. Biol Chem 15: 3287-93.

Jeziorski, M.C., Greenberg, R.M. and Anderson, P.A. (2000). The Molecular Biology of Invertebrate Voltage-gated Ca^{2+} channels. J. Exp. Bio. 203: 841-856.

Jeziorski, M.C., Greenberg, R.M., Clark, K.S., Anderson, P.A. (1998). Cloning and functional expression of a voltage-gated calcium channel alpha1 subunit from jellyfish. J. Biol. 273: 22792-9.

Kerr, R. (2002). Imaging Excitable Cell Activity in *C.elegans*. University of California, San Diego. Dissertation.

Kerr, R., Lev-Ram, V., Baird, G., Vincent, P., Tsien, R.Y., Schafer, W.R. (2000). Optical imaging of calcium transients in neurons and pharyngeal muscle of C.elegans. Neuron 26: 583-94.

Klugbauer, N., Lacinová, L., Marais, E., Hobom, M. and Hofmann, F. (1999). Molecular Diversity of the Calcium Channel $\alpha_2\delta$ Subunit. J. Neuroscience 19: 684-691.

Lakowicz, J.R. "Principles of Flourescence Spectroscopy". 1983. Plenum Press

Lee, R.Y.N., Lobel, L., Hengartner, M., Horvitz, H.R. and Avery, L. (1997). Mutations in the alpha1 subunit of an L-type voltage-activated Ca^{2+} channel cause myotonia in Caenorhabditis elegans. EMBO 16: 6066-6076.

Letts, V.A., Felix, R., Biddlecome, G.H., Arikkath, J., Mahaffey, C.L., Valenzuela, A., Bartlett, F.S. 2nd, Mori, Y., Campbell, K.P., Frankel, W.N. (1998). The mouse stargazer gene encodes a neuronal Ca^{2+}-channel gamma subunit. Nature Genetics 19: 340-7.

Mangano TJ, Patel J, Salama AI, Keith RA. (1991). Inhibition of K(+)-evoked [3H]D-aspartate release and neuronal calcium influx by verapamil, diltiazem and dextromethorphan: evidence for non-L/non-N voltage-sensitive calcium channels. Eur J Pharmacol.192:9-17

Marais, E., Klugbauer, N. and Hofmann, F. (2001). Calcium Channel $\alpha_2\delta$ subunits – Structure and Gabapentin Binding. Mol. Pharmacol 59:1243-1248.

Martin, D.J., McClelland, D., Herd, M.B., Sutton, K.G., Hall, M.D., Lee, K., Pinnock, R.D., Scott, R.H.(2001). Gabapentin-mediated inhibition of voltage-activated Ca2+

channel currents in cultured sensory neurones is dependent on culture conditions and channel subunit expression. Neuropharmacology. 42: 353-66

Maruyama, T., Kanaji, T., Nakade, S., Kanno, T. and Mikoshiba, K. (1997). 2APB, 2-aminoethoxydiphenyl borate, a membrane-penetrable modulator of Ins(1,4,5)P-3-induced Ca2+ release. Jpn. J. Biochem. 122: 498-505.

Maryon, E.B., Coronado, R. and Anderson, P. (1996). *unc-68* Encodes a Ryanodine Receptor Involved in Regulating *C.elegans* Body-Wall Muscle Contraction. J. Cell Biology. 134: 885-893.

Mello, C. and Fire, A. (1995). DNA transformation. In *Caenorhabditis elegans*: Modern Biological Analysis of an Organism, Methods in Cell Biology, Volume 48, H.F. Epstein and D.C. Shakes, eds. (San Diego, CA: Academic Press), pp. 451-482.

Miller, K.G., Alfonso, A., Nguyen, M., Crowell, J.A., Johnson, C.D., Rand, J.B. (1996). A genetic selection for Caenorhabditis elegans synaptic transmission mutants. Proc Natl Acad Sci USA 93: 12593-8.

Miyawaki, A., Griesbeck, O., Heim, R. and Tsien, R.Y. (1999). Dynamic and quantitative Ca2+ measurements using improved cameleons. Proc. Natl. Acad. Sci. 96: 2135-2140.

Miyawaki, A.., Llopis, J., Heim, R.., McCaffery, J.M., Adams, J.A., Ikura, M. and Tsien, R.Y. (1997). Flourescent indicators for Ca^{2+} based on green flourescent proteins and calmodulin. Nature 388: 882 – 887.

Nakai, J., Dirksen, R.T., Nguyen, H.T., Pessah, I.N., Beam, K.G. and Allen, P.D. (1996). Enhanced dihydropyridine receptor channel activity in the presence of ryanodine receptor. Nature 380: 72-75.

Neher, E. (1995). The Use of Fura-2 for Estimating Ca buffers and Ca fluxes. Neuropharmacology 34: 1423-1442.

Nguyen, M., Alfonso, A., Johnson, C.D., Rand, J.B. (1995). Caenorhabditis elegans mutants resistant to inhibitors of acetylcholinesterase. Genetics 140: 527-35.

Nickell, W.T., Pun, R.Y.K., Bargmann, C.I. and Kleene, S.J. (2002). Single Ionic Channels of Two Caenorhabditis elegans Chemosensory Neurons in Native Membrane. J. Membrane Biol. 189: 55-66.

Pozzan, T., Arslan, P., Tsien, R.Y. and Rink, T.J. (1982). Anti-Immunoglobulin, Cytoplasmic Free Calcium, and Capping in B Lymphocytes. J. Cell Biology 94: 335-340.

Ren, D., Navarro, B., Xu, H., Yue, L., Shi, Q. and Clapham, D.E. (2001). A prokaryotic voltage-gated sodium channel. Science 294: 2371-2375.

Schafer, W.R., Sanchez, B.M., Kenyon, C.J. (1996). Genes affecting sensitivity to serotonin in Caenorhabditis elegans. Genetics 143:1219-30.

Schramm, M., Thomas, G., Towart, R. and Franckowiak, G. (1983). Activation of calcium channels by novel 1,4-dihydropyridines. A new mechanism for positive ionotropics or smooth muscle stimulants. Arzneimittelforschung 33:1268-72.

Singer, D., Biel, M., Lotan, I., Flockerzi, V., Hofmann, F., Dascal, N. (1991). The roles of the subunits in the function of the calcium channel. Science 253: 1553-7.

Striessnig, J., Grabner, M., Mitterdorfer, J., Hering, S., Sinnegger, M.J. and Glossman, H.. (1998). Structural basis of drug binding to L Ca2+ channels. Trends Pharm. Sci. 19: 108-115.

Sutton, K.G., Martin, D.J., Pinnock, R.D., Lee, K., Scott, R.H. (2002). Gabapentin inhibits high-threshold calcium channel currents in cultured rat dorsal root ganglion neurones. Br. J. Pharmacology 135:257-265.

Tam, T., Mathews, E., Snutch, T.P. and Schafer, W.R. (2000). Voltage-Gated Calcium Channels Direct Neuronal Migration in Caenorhabditis elegans. Dev. Biology 226: 104-117

Tavernarakis, N. and Driscoll, M. (1997). Molecular Modeling of Mechanotransduction in the Nematode Caenorhabditis Elegans. Annu. Rev. Physiol. 59: 659-689.

The C. elegans Sequencing Consortium. (1998). Genome sequence of the nematode C. elegans: a platform for investigating biology. Science 282: 2012-8

Thomas, D., Tovey, S.C., Collins, T.J., Bootman, M.D., Berridge, M.J., Lipp, P. (2000). A comparison of fluorescent Ca2+ indicator properties and their use in measuring elementary and global Ca2+ signals. Cell Calcium 28: 213-23.

Thomas, J.H. and S. Lockery. 1999. Neurobiology. In "*C. elegans:* a Practical Approach", ed. I. Hope, Oxford University Press.

Tsien, R.Y. and Pozzan, T. (1989). Measurement of Cytosolic Free Ca^{2+} with Quin 2. Methods in Enzymology 172: 230-262.

Tsien, R.Y. and Rink, T.J. (1983). Measurement of Free Ca^{2+} in Cytoplasm. Current Methods in Cellular Neurobiology. Vol 3. pp 249 – 312. Wiley and Sons.

Wang, M., Offord, J., Oxender, D.L. and Su, T.-Z. (1999). Structural requirement of the calcium-channel subunit $\alpha_2\delta$ for gabapentin binding. Biochem. J. 342: 313-320.

White, J.G., Southgate, E., Thomson, J.N. and Brenner, S., F.R.S. (1986). The Structure of the Nervous System of the Nematode *Caenorhabditis elegan*. Phil. Trans. London 314: 1-340.